DEVELOPMENT AND APPLICATION OF TIME DEPENDENT EULER CODE FOR TWO-DIMENSIONAL AND AXISYMMETRIC INTERNAL FLOWS

by

SYED WAJAHAT AZIM

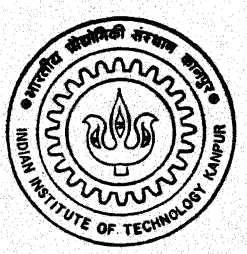

DEPARTMENT OF AEROSPACE ENGINEERING

INDIAN INSTITUTE OF TECHNOLOGY KANPUR

JANUARY, 1996

DEVELOPMENT AND APPLICATION OF TIME DEPENDENT EULER CODE FOR TWO-DIMENSIONAL AND AXISYMMETRIC INTERNAL FLOWS

A Thesis submitted in the partial fulfillment of the requirements for the degree of

MASTER OF TECHNOLOGY

in

AEROSPACE ENGINEERING

by

Syed Wajahat Azim

to the

Department of Aerospace Engineering

Indian Institute of Technology, Kanpur, India

January 1996

AE-1996-M-ARI-D

DEDICATED TO

MY

PARENTS

WHO SACRIFICED

SO MUCH

SO THAT

I COULD GET A DECENT EDUCATION

CERTIFICATE

It is certified that the work presented in this report entitled "Development and Application of a Time Dependent Euler Code for Two-Dimensional and Axisymmetric Internal Flows" by S. W. Azim has been carried out under my supervision in partial fulfillment of the requirements for the award of M.Tech. degree in Aerospace Engineering. This report is a record of bonafide work carried out in the department of Aerospace Engineering, Indian Institute of Technology, Kanpur during the year 1994-95 and this work has not been submitted elsewhere for a degree.

Dr. R. K. Sullerey
Professor
Department of Aerospace Engg.
Indian Institute of Technology,Kanpur
India 208016

January 1996

ACKNOWLEDGEMENTS

I wish to place on record my gratitude to my thesis supervisor Dr. R. K. Sullerey, Professor, Department of Aerospace Engineering, Indian Institute of Technology, Kanpur. His encouraging attitude like a friend and protective posture of a father has been of immense help during the M.Tech. program. This personalized attention & care has helped me regain my confidence which I had lost in the undergraduate program.

I am also thankful to the help given by Mr. U. S. Dixit, a mechanical engineering Ph.D. scholar and Dr. S. Mittal, Assistant Professor, department of Aerospace Engineering in developing the computer codes for this thesis. Mr. U. S. Dixit has been a constant source of help in debugging the codes. Mr. V. C. Srivastava, Mr. K. Mohan and Mr. A. K. Rajpal have also been very helpful in the typing of the thesis and I am thankful to them.

S. W. Azim

Department of Aerospace Engg.

Indian Institute of Technology

Kanpur, India

January 1996

CONTENTS

List of Figures

NOMENCLATURE

Symbol	Description
B_X	airfoil axial chord
C_{pi}	pressure coefficient
e	total energy
L_e	divergent length of B3 nozzle
N_e	number of nodes
p	static pressure
R	radius
R_a	nozzle inlet height
ψ	shape function
superscript	
e	elemental value
n	value at the n^{th} time step
o	stagnation value
T	transpose
subscript	
h	discrete approximation of the variable

ABSTRACT

Euler codes have been developed to study axisymmetric and two-dimensional internal flows . A time-dependent approach has been used to predict steady state flowfields. The steady state solution is achieved asymptotically. The method is based on backward finite differencing in time. A least-squares finite element scheme for first order systems of partial differential equations in space is applied to the Euler equations. The scheme minimizes the L^2 -norm of the residual within each time step. The method naturally generates numerical dissipation proportional to the time-step. An implicit method employing linear elements has been implemented and has proved robust. Three separate codes have been developed and validated for 2-D case in non-conservative variables, 2-D conservative variables and axisymmetric case. The various cases that have been tried include shock reflection from a wall, supersonic flow over a ramp, two-dimensional nozzle with supersonic inlet flow, 2-D mixed flow nozzle with and without shocks, axisymmetric nozzles and flow through a turbine cascade. Flowfields in some of the cases involved both the subsonic and supersonic regimes. The shock capturing capability of the codes has also been demonstrated. The results have been compared wherever possible with experimental or

computational results from various sources and good correspondence has been obtained. The method is computationally expensive especially when shocks are involved or when the grid is relatively fine. Matrix solvers like Gauss elimination, Cholesky's LDL^T factorization method as well as frontal solver were used. Frontal solver reduced the RAM requirements but increased disk space requirement in comparison to the Cholesky's method but there was no appreciable time saving observed between the two for smaller systems.

CHAPTER 1

INTRODUCTION

Propulsion problems encountered in the real life are complex due to interplay of heat and mass transfer, fluid mechanics, chemical kinetics, thermodynamics and turbulence. Such problems are not tractable analytically. It is in this context that numerical methods have assumed eminence. Potential of numerical methods could be exploited when algorithms are developed and chosen judiciously as well as adequately and fast computing system is available.

The internal flows encountered in different components of a propulsion system such as intakes, nozzles and turbomachinery cascade flows are frequently characterized by mixed subsonic and supersonic regimes and at times presence of shocks. Such flow fields cannot be studied by either method of characteristics or finite difference space marching technique due to mixed nature of the flow. Time marching technique has been used for quite some time now to simulate such flowfields because it renders the equations hyperbolic with respect to time and so for the entire domain of interest the nature of equations remains the same. The pseudo-transient is used to obtain the steady state results.

The Navier-Stokes equations govern the flows commonly encountered in both internal and external applications. Computing a

solution of the Navier-Stokes equations is frequently impossible or atleast impractical and in many of these applications, unnecessary. For sufficiently large Reynolds numbers the important viscous effects are confined to a thin boundary layer near the surface of a solid boundary. As a consequence , the inviscid (non-viscous, non-conducting) portion of the flowfield can be solved independently of the boundary layer. Ofcourse this is only true if the boundary layer is very thin compared to the characteristic length of the flowfield so that the interaction between the boundary layer and the inviscid portion of the flowfield is negligible. The reduced set of equations valid only in the inviscid portion of the flowfield, obtained by dropping both the viscous terms and the heat transfer terms from the complete Navier-Stokes equations can be numerically solved using much less computer time than is required for the complete Navier-Stokes equations. These equations are referred to as the Euler equations. In the present investigation a few typical propulsion problems involving internal flows have been studied using time dependent finite element method. Euler equations have been solved numerically based on the least-squares formulation.

1.1> LITERATURE SURVEY

A.> FINITE DIFFERENCE AND FINITE VOLUME TIME MARCHING TECHNIQUES

In a mixed flow flow field the nature of equations changes from elliptic to hyperbolic or vice-versa and this creates difficulties in the numerical solutions. Hence time dependent method is frequently used to analyze such flow fields. The time dependent method uses a pseudo-transient approach whereby the steady state is obtained asymptotically. Using this approach the equations remain hyperbolic with respect to time for both subsonic as well as supersonic regimes and so the difficulties faced previously are avoided. Very efficient shock capturing schemes have been developed for these equations for internal and external flows. The discontinuities are obtained as part of the solution. The advantages of time marching are:

1.> The same code works for the all flow regimes whether subsonic or hypersonic, viscous or inviscid;

2.> The technique can be easily implemented and modified for use on parallel computers;

3.> The same computer program can be used to analyze internal as well as external flows by using the appropriate boundary conditions; and

4.> For complex flow geometries and flow fields the technique is robust.

The time marching schemes can be either explicit and implicit. The Lax -Wendroff scheme and its variants were the first explicit schemes to be developed. After this came the predictor-corrector scheme of MacCormack [1] . Jameson developed and implemented the Runge-Kutta multistage methods for Euler equations in 1981 [1]. This method is especially attractive when implemented with implicit residual averaging, local time-stepping and multi-grid finite volume formulation. In case of implicit schemes the time-step is not restricted by the CFL limit. A comparison between the explicit and implicit schemes for turbomachinery flows by Hall [1] showed that the Runge-Kutta method gives slightly better performance as the artificial viscosity is introduced and controlled by the user.

B.> FINITE ELEMENT METHODS

One of the major problems faced in finite difference and finite volume methods in CFD is the generation of grids for three dimensional geometries realistic geometries of aerospace vehicles. The generation of a single grid that discretizes the entire flow region for a complex region is a very complicated task. Even for axi-symmetric geometries structured grid generation for multiple connected domains such as that of an airbreathing

rocket, often leads to problems such as improper resolution in some regions and excessive grids in some other regions. These difficulties have led to recent research into alternate approaches for handling complex geometries such as zonal approach, unstructured finite volume and unstructured finite element approaches.

Finite element methods are rather new to CFD and hence immature for flowfield analysis in comparison to finite difference method. The finite element method was originally developed by aircraft structural engineers in 1950's to analyze large systems of structural elements in the aircrafts. Turner, Clough, Martin and Topp presented the first paper on the subject, followed by Clough and Argyris , among others [2]. Applications of finite element method to non-structural problems such as fluid flows was initiated by Zienkiewicz [2].

Today various theories of fluid behavior are available which encompass virtually any type of phenomena of much immediate practical interest. However, there remains a surprising number of unsolved important problems in fluid dynamics due to difficulties encountered in most of the conventional analytical and numerical methods. In fluid dynamics, a choice of Eulerian coordinates renders the resulting governing equations non-linear, in general, and thus analytically difficult to solve. The most widely used numerical method of overcoming these

difficulties has been the method of finite differences. Among other popular methods are the variational methods and methods of weighted residuals. Unfortunately, variational principles often cannot be found in some engineering problems, particularly when the differential equations are not self-adjoint. Weighted residuals are applied in the methods of Galerkin, Least-squares, and Collocation. In case of least-squares method, the physical behavior of the system is generally described by linear or lower order functions.

The success of upwind finite differencing and related artificial dissipation methods motivated studies of analogous upwind finite element methods; similarly, the idea of the Lax-Wendroff scheme in finite differencing has motivated studies of Taylor-Galerkin finite element algorithms. For example, the streamline upwind Petrov-Galerkin method [3], the Taylor-Galerkin method [4-6], the Taylor-Galerkin method with flux-corrected transport (FCT) [7-9], block relaxation via Godunov's method [10] and the characteristic Galerkin method [11] have been developed and applied with considerable success to these problems. Recently attempts are being made on the parallelisation of Finite Element programs to increase the overall efficiency of the computation [12].

In the least-squares method, generally linear order elements are used and they give reasonable results. Moreover, the stiffness matrix

produced for least-squares formulation is symmetric and positive definite so matrix solvers like the Cholesky's method can be used resulting in the program being more efficient. Jiang and Carey [13] have used the time-dependent version of this method on Euler equations and demonstrated its robustness in shock capturing.

1.2> PRESENT INVESTIGATION

In the present investigation, three separate codes have been developed based on Ref.[13]. These codes are modular in nature and hence easily alterable as and when necessary. They are capable of simulating both external as well as internal flows, depending on the boundary conditions. The codes have been developed for:

a.) 2D case in non-conservative variables;

b.) 2D case in conservative variables; and

c.) Axisymmetric case in conservative variables.

The code can only simulate inviscid flow fields, being based on Euler equations but can be easily extended to study viscous flow regimes as well. It uses the time-dependent least-squares finite element formulation.

In solving the matrices produced by the formulation Gauss Elimination, Cholesky's LDL^T factorization as well as Frontal solver were used but generally Cholesky's method was used.

A number of steady state cases have been studied. The different problems studied are:

1.) shock reflection problem based on Ref.[13] using the 2D nonconservative variables code;

2.) Supersonic flow over a 20 degree ramp based on Ref.[13] using 2D non-conservative variables code;

3.) B3 nozzle for pressure ratios of 9.0 & 1.98 [1] using the 2D conservative variables code ;

4.) Axisymmetric nozzles [Ref.14,15] without shock using the axisymmetric code;

5.) 2D nozzle with a half angle of 15 degree using the 2D conservative variables code; and

6.) Turbomachinery cascade flow [Ref.16] using the 2D nonconservative variables code .

CHAPTER 2

METHODOLOGY

1. Governing Equations

The compressible Euler equations, which form the basis of this thesis, can be written in conservative form as follows:

$$\frac{\partial U}{\partial t} + \frac{\partial E}{\partial x} + \frac{1}{y^{jo}} \frac{\partial \left(y^{jo} F \right)}{\partial y} = jo \frac{H}{y^{jo}} \qquad (2.1)$$

where $j_o = 0$ or 1 for either two-dimensional or axisymmetric flow, respectively, and

$$U = \begin{bmatrix} \rho \\ \rho u \\ \rho v \\ \rho e \end{bmatrix}; \qquad E = \begin{bmatrix} \rho u \\ \rho u^2 + p \\ \rho uv \\ \rho ue + up \end{bmatrix} \qquad (2.2)$$

$$F = \begin{bmatrix} \rho v \\ \rho uv \\ \rho v^2 + P \\ \rho ve + pv \end{bmatrix}; \quad H = \begin{bmatrix} 0 \\ 0 \\ P \\ 0 \end{bmatrix}$$

The conservation form (or conservative variables) implies that the partial differential equations (PDE) having this form have the property that the coefficients of the derivative terms are either constant or, if variable, their derivatives appear nowhere in the equation. For a PDE which represents a physical conservation statement, this means that the divergence of a physical quantity can be identified in the equation. In Navier-Stokes

equations when the dependent variables are in the form:

$$\rho\ ,\ \rho u\ ,\ \rho v\ ,\ \rho e$$

then the equation is said to be in conservative form. On the other hand, if the dependent variables are: $\rho\ ,\ u\ ,\ v\ ,\ e$ then the equation is said to be in non-conservative form. The finite representations of the PDE should be such that a good approximation of the conservation laws implied by the PDE is maintained. Almost all the finite element analogs can be generally assured of the conservative property because of the very nature of the control volume built into the integral formulation in FEM.

2.> Technique

The steady supersonic flowfields are governed by hyperbolic differential equations, whereas steady subsonic flowfields are described by elliptic differential equations.

There are various cases where the internal and/or external flow involves both the subsonic and supersonic regimes. Flows through converging-diverging nozzle and over a blunt body may involve both the regimes. The fact that the nature of the governing equations changes from elliptic to hyperbolic across the sonic line causes severe mathematical and numerical difficulties at such a level that steady flow

solution of the subsonic and supersonic regimes are usually treated separately and differently. The time marching technique for the solution of steady flows was developed in 1966 by Moretti and Abbett [20], which was published as the first practical solution for the supersonic blunt body problem. Since then time-marching also called as time dependent solutions have become an important segment of computational fluid dynamics.

The unsteady equations of motion are Hyperbolic with respect to time, regardless of the fact whether the flow is locally subsonic or supersonic. Hence the flowfields lend themselves to a well posed initial value problem with respect to time. Therefore, the time marching technique becomes very powerful tool for the solutions of such mixed flows, being uniformly valid throughout the flowfield.

In flowfields involving shock waves, there are sharp, discontinuous changes in the primitive flowfield variables such as pressure, density, velocity, temperature etc. across the shocks. Many computations of the flows with shocks are designed to have the shock waves appear naturally within the computational space as a direct result of the overall flowfield solution, i.e. as a direct result of the general algorithm, without any special treatment to take care of shocks themselves. Such approaches are called shock capturing methods. This

is in contrast to the alternate approach, where shock waves are explicitly introduced into the flowfield solution, the exact Rankine-Hugonoit relations for changes across shock are used to relate the flow immediately ahead of and behind the shock, and the governing flow equations are used to calculate the remainder of the flowfields. This approach is called the shock fitting method.

The shock fitting technique often breaks down when shocks develop spontaneously within the fluid.

Here a time dependent finite element method with shock capturing has been used. Finite element methods are well suited to practical problems posed on the complicated domains and are now extensively applied in solid mechanics, heat transfer, fluid flow etc. The earlier difficulties encountered in extending the methodology beyond elliptic boundary value problems and to convection dominated flows have been substantially resolved. Here we begin by considering the backward implicit time differenced formulation.

3. Mathematical formulation

The three different cases of two-dimensional non-conservative variables, two-dimensional conservative variables and axisymmetric conservative variables are treated separately as follows:

a.> The two-dimensional non-conservative case[13]: The two-dimensional unsteady compressible Euler equations in non-conservative form can be represented as a first-order system as:

$$\frac{\partial U}{\partial t} + A_1 \frac{\partial U}{\partial x} + A_2 \frac{\partial U}{\partial y} = 0 \quad \text{in } \Omega \text{ x } (0,T),$$

$$MU = g \qquad \text{in } \Gamma_g \text{ x } (0,T), \qquad (2.3)$$

$$U = U_0 \qquad \text{in } \Omega \text{ for t} = 0$$

where $U^T = (\rho \quad u \quad v \quad p)$, M is a boundary operator, g is a given vector-valued function, Γ_g is that part of the boundary Γ where essential boundary conditions are applied, Ω is the spatial domain of the problem, t is time and

$$A_1 = \begin{bmatrix} u & \rho & 0 & 0 \\ 0 & u & 0 & \rho^{-1} \\ 0 & 0 & u & 0 \\ 0 & \gamma p & 0 & u \end{bmatrix} \qquad (2.4)$$

$$A_2 = \begin{bmatrix} v & 0 & \rho & 0 \\ 0 & v & 0 & 0 \\ 0 & 0 & v & \rho^{-1} \\ 0 & 0 & \gamma p & v \end{bmatrix}$$

Here ρ is the density, (u,v) are the velocity components, p is the pressure and γ is the specific heat ratio.

For a given time step $\Delta t = t^{n+1} - t^n$ we linearize the problem by setting $A_1=A_1(U^n)$, $A_2 = A_2(U^n)$. Backward differencing leads to the implicit time-differenced problem

$$U^{n+1} - U^n + \Delta t A_1^n \frac{\partial U^{n+1}}{\partial x} + \Delta t A_2^n \frac{\partial U^{n+1}}{\partial y} = 0 \qquad (2.5)$$

Introducing $\Delta U = U^{n+1} - U^n$ we rewrite the above equation as

$$\Delta U + \Delta t A_1^n \frac{\partial \Delta U}{\partial x} + \Delta t A_2^n \frac{\partial \Delta U}{\partial y} + \Delta t \left(A_1^n \frac{\partial U^n}{\partial x} + A_2^n \frac{\partial U^n}{\partial y} \right) = 0 \quad (2.6)$$

The basic least-squares method for the system (2.6) amounts to minimizing the L^2 - norm of the residual R for admissible ΔU in (2.6); i.e. minimizing the objective functional

$$\Phi_0 = \int_\Omega R^T R \, dx dy \qquad (2.7)$$

with

$$R = \left[\Delta U + \Delta t A_1^n \frac{\partial \Delta U}{\partial x} + \Delta t A_2^n \frac{\partial \Delta U}{\partial y} + \Delta t \left(A_1^n \frac{\partial U^n}{\partial x} + A_2^n \frac{\partial U^n}{\partial y} \right) \right] \quad (2.8)$$

Taking variations with respect to ΔU and setting the test function $V = \delta\Delta U$, $\delta\Phi_0 = 0$ leads to the least-squares weak statement: find $\Delta U \in S = \{H^1(\Omega); M(\Delta U) = 0 \quad on \quad \Gamma_g\}$, where $H^1(\Omega)$ denotes the usual Hilbert space, such that

$$\int_\Omega \left[V + \Delta t A_1^n \frac{\partial V}{\partial x} + \Delta t A_2^n \frac{\partial V}{\partial y}\right]^T \left[\Delta U + \Delta t A_1^n \frac{\partial \Delta U}{\partial x} + \Delta t A_2^n \frac{\partial \Delta U}{\partial y} + \Delta t\left(A_1^n \frac{\partial U^n}{\partial x} + A_2^n \frac{\partial U^n}{\partial y}\right)\right] dx dy = 0$$

$$\forall \quad V \in S \tag{2.9}$$

Next we introduce a finite element discretization. Let N_e be the number of nodes for an element and Ψ_j denote the element basis functions. The approximation and the test function are

$$\Delta U_h(x,y) = \sum_{j=1}^{N_e} \varphi_j(x,y) E \Delta \begin{bmatrix} \rho \\ u \\ v \\ p \end{bmatrix}_j \tag{2.10}$$

$$V_h(x,y) = \Psi_i(x,y)E \tag{2.11}$$

where $\Delta(\rho,u,v,p)_j^T$ are the nodal values at the j^{th} node and E is the 4x4 identity matrix. Substituting ΔU_h, V_h for ΔU, V in (2.9) and evaluating the integrals, we have

$$K(\Delta U) = F \tag{2.12}$$

where ΔU is the global nodal vector. The global matrix K and the global vector F are assembled from the following submatrices and subvectors respectively:

$$K_{ij}^{e} = \int_{\Omega^e} (L\varphi_i)^T L\varphi_j \, dxdy \qquad (2.13)$$

$$F_i^e = -\int_{\Omega^e} (L\varphi_i)^T \Delta t \left(A_1^n \frac{\partial U^n}{\partial x} + A_2^n \frac{\partial U^n}{\partial y} \right) dxdy \qquad (2.14)$$

where $L\varphi_i = \varphi_i E + \Delta t \varphi_{i,x} A_1^n + \Delta t \varphi_{i,y} A_2^n$

It can be noted that the stiffness matrix K is symmetric, positive and definite. This is an important feature of the least-squares method. Only the lower half matrix need be generated and stored if Cholesky LDL^T factorization is used.

b.> Two-Dimensional conservative form[13]: The Euler equations governing two-dimensional compressible inviscid flows can be written in conservative form as:

$$\frac{\partial Q}{\partial t} + \frac{\partial F}{\partial x} + \frac{\partial G}{\partial y} = 0 \quad \text{in } \Omega \text{ x } (0,T),$$

$$MQ = g \quad \text{in } \Gamma_g \text{ x } (0,T), \qquad (2.15)$$

$$Q = Q_0 \quad \text{in } \Omega \text{ for } t = 0$$

where

$$Q = \begin{bmatrix} \rho \\ \rho u \\ \rho v \\ \rho e \end{bmatrix}$$

$$F = \begin{bmatrix} \rho u \\ \rho u^2 + p \\ \rho u v \\ \rho u e + u p \end{bmatrix} \qquad (2.17)$$

$$G = \begin{bmatrix} \rho v \\ \rho u v \\ \rho v^2 + p \\ \rho v e + p v \end{bmatrix}$$

in which e is the total energy and for the case of a perfect gas the equation of state is

$$p = (\gamma - 1)\left[\rho e - \frac{1}{2}\rho\left(u^2 + v^2\right)\right] \qquad (2.17)$$

Now we convert this to the following modified form:

$$\frac{\partial Q}{\partial t} + A_1 \frac{\partial Q}{\partial x} + A_2 \frac{\partial Q}{\partial y} = 0 \qquad (2.18)$$

It has to be noted that the A-matrices (both 1 & 2) in this case are different from those of the non-conservative case. The new A-matrices are given below:

$$A_1 = \begin{bmatrix} 0 & 1 & 0 & 0 \\ \frac{1}{2} g b \left(u^2 + v^2\right) - u^2 & (3 - \gamma) u & - g b \cdot v & g b \\ - u v & v & u & 0 \\ \left[g b \left(u^2 + v^2\right) - \gamma e\right] u & e b - u^2 g b & - g b \cdot u v & \gamma u \end{bmatrix}$$

$$A_2 = \begin{bmatrix} 0 & 0 & 1 & 0 \\ - u v & v & u & 0 \\ \frac{1}{2} g b \left(u^2 + v^2\right) - v^2 & - g b \cdot u & (3 - \gamma) v & g b \\ \left[g b \left(u^2 + v^2\right) - \gamma e\right] & - g b \cdot u v & e b - g b \cdot v^2 & \gamma v \end{bmatrix} \qquad (2.19)$$

in which $gb = \gamma - 1, \quad eb = \gamma e - gb\left(\frac{u^2 + v^2}{2}\right)$

Using the same procedure as before, we construct a corresponding least-squares weak statement similar to (27) where the matrix operators in (23),(24) are again evaluated at the previous time level. This implies that an approximate conservative form can be reconstructed. We have the a conservative least-squares weak statement:

find $\Delta Q \in S = \left\{\left(H^1(\Omega)\right)^4; M(\Delta Q) \le 0 \quad on \quad \Gamma_g\right\}$ such that

$$\int_\Omega \left[V + \Delta t A_1^n \frac{\partial V}{\partial x} + \Delta t A_2^n \frac{\partial V}{\partial y}\right]^T \left[\Delta Q + \Delta t A_1^n \frac{\partial \Delta Q}{\partial x} + \Delta t A_2^n \frac{\partial \Delta Q}{\partial y} + \Delta t\left(A_1^n \frac{\partial Q^n}{\partial x} + A_2^n \frac{\partial Q^n}{\partial y}\right)\right] dx dy = 0$$

$$\forall \quad V \in S \qquad (2.20)$$

here $\frac{\partial F^n}{\partial x} = A_1^n \frac{\partial Q^n}{\partial x}, \quad \frac{\partial G^n}{\partial y} = A_2^n \frac{\partial Q^n}{\partial y}$

The unknown here is ΔQ, which is the increment in conservative variables for time step Δt. We may use the conservative variables at the previous time step to calculate the nodal values of components of flux F^n and G^n.

c.> The Conservative Axisymmetric case: For this case the equations are as follows:

$$\frac{\partial Q}{\partial t} + \frac{\partial F}{\partial x} + \frac{1}{y}\frac{\partial (y G)}{\partial y} = \frac{H}{y} \qquad (2.21)$$

$$Q = \begin{bmatrix} \rho \\ \rho u \\ \rho v \\ \rho e \end{bmatrix}$$

$$F = \begin{bmatrix} \rho u \\ \rho u^2 + p \\ \rho u v \\ \rho u e + u p \end{bmatrix} \qquad (2.22)$$

$$G = \begin{bmatrix} \rho v \\ \rho u v \\ \rho v^2 + p \\ \rho v e + p v \end{bmatrix}$$

$$H = \begin{bmatrix} 0 \\ 0 \\ p \\ 0 \end{bmatrix}$$

Here again almost the same analysis as that of the case (b) is repeated. Pressure P is represented by:

$$p = (\gamma - 1)\begin{bmatrix} \rho & \rho u & \rho v & \rho e \end{bmatrix}\begin{bmatrix} 0 \\ -\frac{1}{2}u \\ -\frac{1}{2}v \\ 1 \end{bmatrix} \qquad (2.23)$$

$$\frac{\partial Q}{\partial t} + \frac{\partial F}{\partial x} + \frac{\partial G}{\partial y} + \frac{(G - H)}{y} = 0 \qquad (2.24)$$

The above equation can be reduced to the following form:

$$\frac{\partial Q}{\partial t} + A_1 \frac{\partial Q}{\partial x} + A_2 \frac{\partial Q}{\partial y} + \frac{(G - H)}{y} = 0 \qquad (2.25)$$

When the analysis is carried on the above equation the first three terms are treated as in the 2-D conservative variable case. Only the third new term has also to be taken into account. The A_1 and A_2 matrices are the same as in the case (b). Here the residual R is

$$R = \left[\Delta Q + \Delta t A_1^n \frac{\partial \Delta Q}{\partial x} + \Delta t A_2^n \frac{\partial \Delta Q}{\partial y} + \Delta t \left(A_1^n \frac{\partial Q^n}{\partial x} + A_2^n \frac{\partial Q^n}{\partial y} \right) \right] + \frac{\Delta t v}{y} \left(\Delta Q + Q^n \right)$$

$$+ \frac{\Delta t v (\gamma - 1) MS}{y} \left(\Delta Q^T + Q^{nT} \right) \qquad (2.26)$$

The M and S matrices are as follows:

$$M = \begin{bmatrix} 0 \\ -\frac{1}{2}u \\ -\frac{1}{2}v \\ 1 \end{bmatrix} \qquad S = \begin{bmatrix} 0 \\ 0 \\ 0 \\ 1 \end{bmatrix} \qquad (2.27)$$

Now again minimizing the L^2 -norm we get the corresponding weak form and thereby the K and F matrices.

CHAPTER 3

A NOTE ON THE COMPUTER PROGRAM

The mathematical formulation has already been discussed in the last chapter. Utilizing that formulation three separate codes have been developed. These codes are modular in nature and as such with the exception of a few subroutines the codes are same for all three cases. Given below is a listing of the subroutines along with the function of each for the convenience of any prospective user. In all there are 16 subroutines:

1.> NODEDT : In this subroutine the geometry of the domain is specified and it generates the nodes and the connectivity matrix. Here the number of nodes and the number of elements is supplied.

2.> INITDT : In this subroutine the initial values of the dependent variables are specified and the number and location of the gauss points has to be given for numerical integration. The weights for different orders of integration at different gauss points are also given.

3.> WAJAZ : This subroutine is called from the subroutine ELEMENT. It supplies a component of the elemental stiffness matrix at a particular gauss point. It has to be supplied the number of element being

computed and the gauss point for which the value is being presently calculated.

4.> SABAZ : This subroutine is also called from the ELEMENT. This requires the element number and the gauss point and gives the value of the elemental force vector at this location.

5.> MULT : This subroutine is simply for multiplication of different matrices required in the computation of elemental force and stiffness vectors.

6.> TRANS : This subroutine simply gives the transpose of the matrix supplied to it.

7.> ERROR : This subroutine is called from different subroutines if there is an error. It prints an error message. For example, when the jacobian becomes equal to zero (which it should not be) or when the global stiffness matrix which should be symmetric but is not due to some error.

8.> GKSS : This subroutine is one of the most important one's. It generates the elemental force and stiffness matrices by calling ELEMENT and then assembles them to yield the global stiffness and force matrices.

9.> SHAPE : This subroutine supplies the shape functions for the four noded quadrilaterals that have been used in this analysis.

10.> JACOBI : This supplies the jacobian for the isoparametric transformation of the elements and also checks that the jacobian is not zero otherwise it would imply that there has been faulty grid generation.

11.> ELEMENT : This subroutine has already been mentioned above and it is called from GKSS. It requires the element number. It does the numerical integration and supplies the elemental stiffness and force matrices.

12.> APLYBC : As is obvious from its name, this subroutine applies the boundary conditions.

13.> CALFUN : This subroutine calls the matrix solver like the gauss elimination or the Cholesky's factorization, as the case maybe.

14.> PRINTS : This one prints the results. All the computed variables are supplied to this subroutine through the common block and whichever is desired can be printed.

15.> CHOLDC : This is a part of the two subroutines that do the Cholesky's factorization and then solve the matrix. This does the decomposition part.

16.> CHOLSH : This solves the matrix to yield the results of the algebraic equations that result from any numerical method.

The time step, maximum number of iterations as well as the tolerance factor are specified in the main program. For different cases (i.e.

whether 2D or axisymmetric, conservative or non-conservative) the subroutines SABAZ and WAJAZ have to be replaced with the appropriate ones. For different geometries the NODEDT will have to be modified. If frontal solver is used then GKSS has to be deleted because frontal solver does the assembly itself and in a different manner.

CHAPTER 4

RESULTS & DISCUSSION

Seven cases have been run using the developed codes for different boundary conditions. They are discussed below in serial order:

a.> Shock Reflection Problem: The isobars for the standard test problem corresponding to the reflection of a shock from a wall are depicted in Fig. 1. On the upper boundary of the flow domain ρ=1.7, u=2.6185, v=-0.5082, p=1.5282 and on the upstream boundary ρ=1.0, u=2.9, v=0.0, p=0.7143, so a shock emanates from the upper left corner. This shock is reflected at the lower wall where v=0 (symmetry condition is applied here) and the downstream boundary conditions remain free for outflow. The initial data were prescribed as constant at values given on the upper boundary and the specific heat ratio is γ=1.4. In the calculation a uniform 60x20 mesh of bilinear elements was used. The solution was integrated with a time step Δt=0.33333 until an essentially steady state was obtained in 26 timesteps. The results were obtained using the 2-D code with non-conservative variables. The isobars indicate that the shock captured is somewhat smeared but the shock angles and the pressure values at the exit (i.e. after the shock reflection has already taken place)

show excellent correspondence with the theoretical results. It can be inferred that the flow modelling has been correctly done. This problem was taken from Ref. 13.

b.> Supersonic Flow over a Ramp: The second case studied has again been taken from Ref.[13]. Here a supersonic flow with a Mach Number of 3, over a 20° ramp has been studied using the 2-D non-conservative variables code. The gas enters with uniform flow conditions through the left boundary of the domain and an oblique shock develops at the root of the ramp. The inlet parameters are $u=3.0, v=0.0, \rho=1.0$ and $p=0.7143$ and the same boundary condition was applied on the upper boundary. The mesh contains 824 bilinear elements and the computed pressure contours are illustrated in Fig. 2. In the calculation the initial data were prescribed as constant at the value given on the left boundary and the time step was $\Delta t=0.33333$. The steady state was obtained in 30 time steps. The result obtained here (for eg. the shock angle and the pressure at the exit) are again in close agreement with the theoretical results, although the shock, as in the previous case, is somewhat smeared.

c.> B3 Nozzle: Fig.3 shows the dimensions of B3 nozzle. This geometry, input data and the experimental data (for comparison) were taken from Ref.[1]. This nozzle was studied for two pressure ratios of 9.0

& 1.98. The velocity components(u&v) and the density are specified at the inlet(ρ=1.0,u=0.21,v=0.0) and the pressure ratio at the outlet(P_o/p=9.0). For the first pressure ratio of 9.0 the flow field has no shock. The analysis was done using 30x30 bilinear elements. The results were obtained using the 2-D conservative variables code in 15 time steps and the time step was the same as in previous case. Fig. 4 shows the Iso-Mach contours and Fig. 5 shows the iso-bars for this case. Figures 6 & 7 show the centre-line and wall pressure distribution respectively. They are in good agreement with the experimental data marked on the figures. Figures 8 & 9 show the centre-line & wall Mach number distributions respectively. The Mach number in actual case must be zero at the wall but since an inviscid code has been used so it is not.

Figures 10 & 11 show the Iso-Mach & iso-bars for the same nozzle but for the pressure ratio of 1.98. At the inlet ρ=1.0,u=0.21,v=0.0 and at the outlet P_o/p=1.98. The time step is again Δt=0.33333 and the results were obtained using the 2-D code in conservative variables. The shock that exists for this pressure ratio at about x=1.2 may not be clear from the above figures but can be clearly observed from the centre-line & wall distributions of Mach number and pressure. For this case figures 12 & 13 show the centreline & wall pressure distributions respectively. In

these figures (12 & 13) the experimental data was available so has been shown on the plots and the two results (computationally obtained and the experimentally obtained ones) indicate a good matching. No results were available for the mach number distributions shown in figures 14 & 15 which illustrate centre-line & wall Mach numbers respectively.

d.> Axisymmetric Nozzle: Fig. 16 shows the nozzle geometry taken from Ref.[15]. $\theta_1=29^\circ$, $Y_B = 1.2$, $\theta_B=30^\circ$,$X_B=3.6$, $Y_E=3.7$ and $X_E=9.4$. This case was run with the pressure ratio $(p/P_o)$of 0.01 and the input uniform flow of Mach number of 0.1. On the wall the flow tangency condition was applied and on the lower boundary the symmetry condition was used. The time step was the same as in all previous cases and 40x10 mesh was used. The results were obtained in 24 time steps. Fig. 17 & 18 show the iso-machs and iso-bars respectively. Wall pressure distribution is shown in Fig. 19. Fig. 20 shows the centre-line pressure distribution. The results from Ref.[15] obtained using a finite volume discretization are also shown alongside and the results are once again in good agreement. In figures 21 & 22 the wall & centre-line Mach. no. distributions are given and they also match properly with the results of Ref.[15].

e.> 2-D Nozzle: Fig. 23 shows the mesh and the geometry used for this nozzle. This was a purely supersonic case with no transition from subsonic to supersonic domain. The mesh was very coarse with only 70

elements which were again bilinear. The half angle was 15°. and the case was run for the inlet pressure (non-dimensional) of 0.71 and the corresponding Mach number with a uniform inlet flow. The results match with one-dimensional results. Fig. 24 shows the wall pressure distribution for this case. Fig. 25 shows the Mach number distributions for different axial stations. The time step used was the same as in previous cases and the solution was obtained in 8 time steps.

f.> TND-2579 Nozzle:The data for this was taken from Ref.[14]. The geometry and the mesh used for this nozzle is shown in Fig.26. This again is a purely supersonic case and the axisymmetric code was used to obtain the results. The specific heat ratio for this case was γ=1.2. The inlet uniform flow had a Mach. no. of 1.05(ρ=1.0,u=1.05,v=0.0). Here a mesh of 35x8 was used. The time step was Δt=0.5 and the solution was obtained in 20 time steps. Fig. 27 & 28 show the centre-line & wall pressure distributions for this case. Fig. 29 shows the centre-line Mach. no. distribution for this nozzle. Fig. 30 shows the wall Mach. no. distribution and for this figure we have method of characteristic results [14] to compare. Once again the comparison is excellent.

g.> Cascade Flow: For this case a mesh of 40x8 was used. The airfoil used has been shown in Fig.31. A typical mesh used in the analysis

of gas turbine cascades has been shown in Fig. 32 (this is not the actual mesh). The time step was $\Delta t=0.33333$ and the steady state was reached in 16 steps. The inlet angle was 44.5° and the outlet flow angle was 21.8°. The cascade pitch was 0.825. The inlet flow Mach. number was 0.32 and the pressure ratio imposed at the exit was the one corresponding to the Mach number of 0.58. A periodic boundary condition was imposed on the portions of the computational domain such as: AB & IH and DE & GF (this implies that the values of the computed variables at the lower boundaries IH & GF are updated by the values at the upper boundaries AB & DE respectively after each iteration). Fig.33 shows the centre-line Mach no. distribution and the results show a good matching with those obtained by the streamline curvature analysis. Fig. 34 shows the pressure coefficient for this case and they appear to be slightly off compared to the results of Ref.[16]. The results from the present analysis depart from those of the Ref.[16] especially near the leading and trailing edges. This may be due to the fact that in the reference quoted above the results have been arrived at by repeating the computation around the edges after an initial inviscid analysis followed by a transitional profile boundary layer and wake analysis.

The results have demonstrated the robustness of the codes. The advantage of the least-squares formulation is that reasonable results can be

obtained by lower order elements. In this formulation artificial viscosity appears naturally and the matrices are symmetric (thereby improving the efficiency of the computation). But alongside the shortcoming in this formulation (L^2) is that it is only first order accurate in time and if we try to improve the accuracy to second order then this may lead to oscillations (since we are investigating steady state cases so time accuracy is not relevant). For higher order elements this formulation may result in the appearance of non-physical oscillations in the solution.

CHAPTER 5

CONCLUSIONS AND SCOPE OF FURTHER WORK

5.1> CONCLUSIONS: In order to predict the internal flowfields Euler codes have been developed based on least-squares finite element method. A time-dependent approach has been used to overcome the problems encountered in studying, computationally, flows involving both subsonic and supersonic regimes. Iso-parametric (bilinear quadrilaterals) elements have been used. The codes were developed for two-dimensional as well as axisymmetric cases. For two-dimensional case , two separate codes were developed, one each for non-conservative variables and conservative variables. The axisymmetric code uses conservative variables.

The 2-D non-conservative variables code was first used on the shock reflection problem. Proper shack capturing took place and the computed results matched well with the theoretical shock angles and the after shock pressure.

The non-conservative 2-D code was also used to study supersonic flow over a ramp. Once again the results showed good correspondence with the theoretical results.

The 2-D conservative variables code was used on the B3 nozzle for two different conditions, one involving shock and the other without it. The results were slightly off but trends were the same in both the cases.

The results for the axisymmetric nozzle, without shock were also in agreement with those of a finite volume analysis [15]. This case also involved both subsonic and supersonic flow speeds.

The axisymmetric code was also run for NASA TND 2579 nozzle. This was a purely supersonic case and the results were matched with method of characteristics results and once again there is very good correspondence.

The 2-D conservative code was used on a two-dimensional nozzle with supersonic inlet conditions. The results were compared with one dimensional analysis and the results were almost the same as the theoretical results.

A subsonic flow through a gas turbine cascade was analyzed using the non-conservative 2-D code and the results were slightly off compared to those of streamline curvature analysis.

The results proved the capability of the codes to predict the flowfields for internal flows, with and without shocks.

5.2.> SCOPE OF FUTURE WORK: The entire analysis so far has been done with bilinear quadrilaterals. The same analysis can be repeated with higher order elements. Same 2-D case can be run for both conservative and non-conservative variables and the results compared. Because of the paucity of time the number of cases tried were limited. More complex cases (for e.g., mixed flow through the turbine cascades) can be tried. Different new geometries can be tried, especially those for which the grid generation is more complicated for e.g. internal compression intakes and hypersonic nozzles with flaps. The use of adaptive grid generation can be made to observe how the quality of results alters. New subroutines can be added to include the viscous effects in the program.

REFERENCES

1. T. Jayachandran,`Application of Finite Element Method in Analyzing Flow Fields of Solid Propellant Air Breathing Rockets' Ph.D. Thesis, Aug. 1993, IIT Kanpur.

2. T. J. Chung, `Finite Element Analysis in Fluid Dynamics', McGraw-Hill International Book Co.,1978

3. T.J.R. Hughes,`Recent progress progress in the development and understanding of SUPG methods with special reference to the compressible Euler and Navier-Stokes equations', Int. Jl. of numerical methods in fluids, 7, pp.1261-1275,1987

4. J.Donea, L. Quartapelle and V. Selmin, `An analysis of time discretization in the finite element solution of hyperbolic problems', Jl. Comput. Phys.,70,pp.463-499,1987.

5. J.Donea, V. Selmin and L. Quartapelle, `Finite element schemes for inviscid compressible flows', Trans. 8th Int. Conf. on structural Mechanics in Reactor Technology, Vol. B, North-Holland, pp. 111-115, 1985

6. A.J. Baker, J. W. Kim, J.D. Freels and J.A. Orzechowski,`On a finite element CFD algorithm for compressible viscous and

turbulent aerodynamic flows', Int. Jl. of numer. methods in fluids, 7,1235-1259,1987

7. J. T. Oden, T. Strouboulis and P. Devloo,`Adaptive finite element methods for high-speed compressible flows', Int. Jl.of numer. methods fluids,7,1211-1228,1987

8. R. Lohner,`FEM-FCT and adaptive refinement schemes for strong unsteady flows', Int. Jl. of numerical. methods in fluids, 7, pp.93-114,1987

9. J. Peraire, K. Morgan and O. C. Zienkiewicz,`Convection dominated problems', in T.E.Tezduyar and T.J.R.Hughes (eds), Numerical Methods for compressible Flows-Finite Difference, Element and Volume Techniques, ASME, New York, 1986, pp. 129-148.

10. R. Glowinski and J. Periaux, ` Finite Element methods for the compressible Euler and Navier-Stokes equations, application to aerospace engineering', First world congr. on Computational Mechanics, Abstracts, Vol. 1,1986.

11. K. W. Mortan,`Characteristic Galerkin methods for hyperbolic problems', in Proc. 5th GAMM conf. on Numerical Methods in FluidMechanics, Rome, 1983.

12. P.W.Grant,J.A.Sharp, M.F.Webster and X. Zhang,`Experiences of parallelising Finite-element Problems in a Functional Style', Software-Practice and Experience, Vol.25(9),pp.947-974,Sept. 1995

13. B. N. Jiang and G. F. Carey,` Least-Squares Finite Element Methods for Compressible Euler Equations', Int. Jl. for Numer. methods in fluids, vol. 10, 1990, pp. 557-568.

14. K. Sudhakar, Bhasker Roy (eds.),`Aerothermodynamics of Internal Flows',Proc. of 6th National Convention of Aerospace Engineers held on Jan.24-25,1991 at IIT Bombay.

15. Jayachandran, M. J. Pandya,`Numerical Heat Transfer and CFD 9 Studies on I860 Based Workstation',ISRO,No. PHC. TR:361/91

16. Z-Q. Ye,`A Systematic Computational Design System for Turbine Cascades, Airfoil Geometry, and Blade-To-Blade Analysis',Trans. of the ASME.,Vol.106,July 1984, pp.598-605

17. G. F, Carey and B. N.Jiang,`Least-squares finite elements for first-order hyperbolic systems', Int. Jl. numerical methods eng.,26,pp.81-93,1988

18. B.N.Jiang and G.F. Carey,` A stable Least-squares finite element method for first-order hyperbolic systems', Int. Jl. of numerical methods fluids, 8,pp. 933-942,1988

19. G. F. Carey and B.N.Jiang,`Least-squares finite elements for convective transport problems', Proc. Ninth SPE symp. on reservoir Simulation, Society of Petroleum Engineers(SPE), Inc., 1987, pp. 253-257.

20. Gino Moretti and M. Abbett,` A time-dependent Computational Method for Blunt Body Flows', AIAA Jl., vol. 4, No.12, Dec. 1966, pp. 2136-2141.

21. B. N. Jiang and G. F. Carey,` Least-squares finite elements for compressible Euler equations', in C. Taylor, W. G. Habashi, M.M. Hafez (eds), Numerical Methods in Laminar and Turbulent Flow, Vol. 5, Pineridge Press, Swansea, 1987, pp. 1460-1464.

22. B.N. Srivastava, M.A. Everett, R. Bozzola,` Computation of Flow Fields in High Solidity and High Angle Cascades Using Euler Equations', AIAA-85-1705

23. J. A. Essers, F. Kafyeke,`Application of a fast Pseudo-Unsteady Method to Steady Transonic Flows in Turbine Cascades',Jl. of Engineering for Power, Trans. of the ASME.,81-GT-124.

24. H. U. Akay, A. Ecer,`Finite Element Analysis of Transonic Flows in Highly Staggered cascades',AIAA-81-0210.

25. K. P. Sarathy,` Computation of Three-Dimensional Flow Fields Through Rotating Blade Rows and Comparison with Experiment', Jl. of Engineering for Power, Trans. of the ASME, 81-GT-121.

26. D. A. Anderson, J. C. Tannehill, R. H. Pletcher,`Computational Fluid Mechanics and Heat Transfer', McGraw-Hill Book Co., 1984.

27. A. Dadone, B. Grossman,`Surface Boundary Conditions for the Numerical Solution of the Euler Equations', AIAA Jl., No.2,Feb.1994.

28. R. C. Mehta, T. Jayachandran, V. M. K. Shastry,`Numerical Solution of the Navier-Stokes Equations Using a Finite Element Method', Inter. Jl. for Numerical Methods in Fluids, Vol.13,1991,pp.481-489.

29. J. H. Mathews,`Numerical Methods for Mathematics, Science and Engineering', Prentice-Hall of India,N.Delhi,1994.

30. E. Hinton, D. R. J. Owen,` Finite Element Programming', Academic Press, 1977.

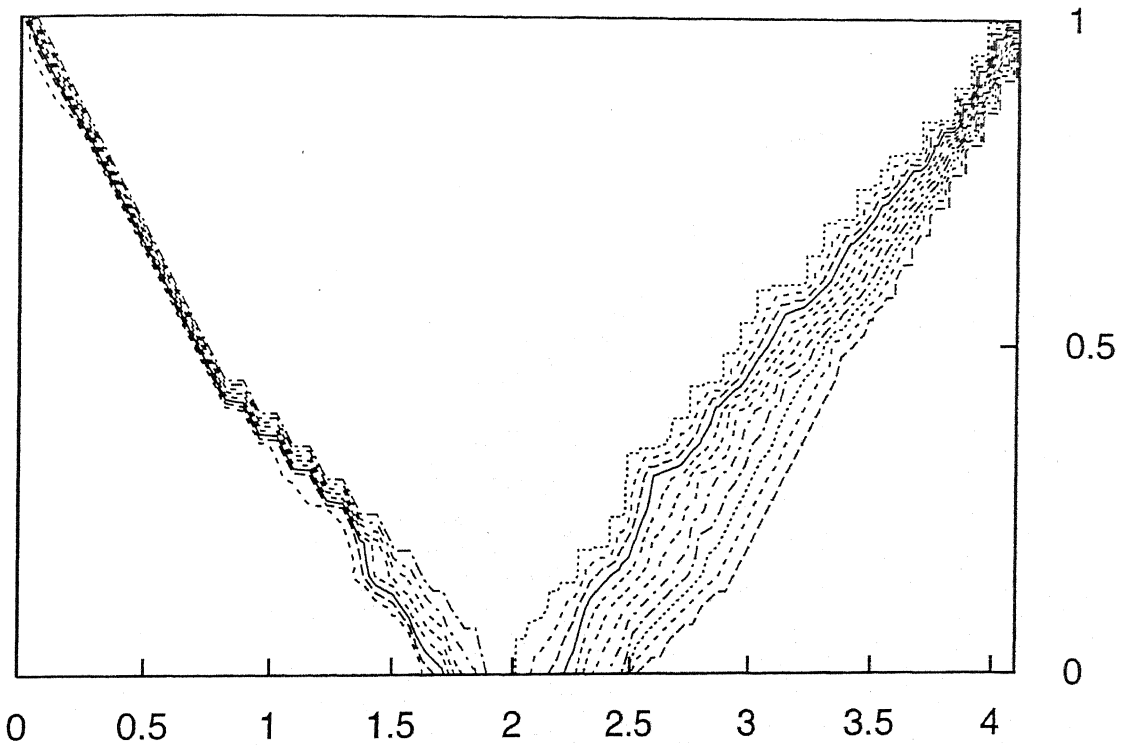

Fig. 1. Iso-bars for Shock Reflection problem

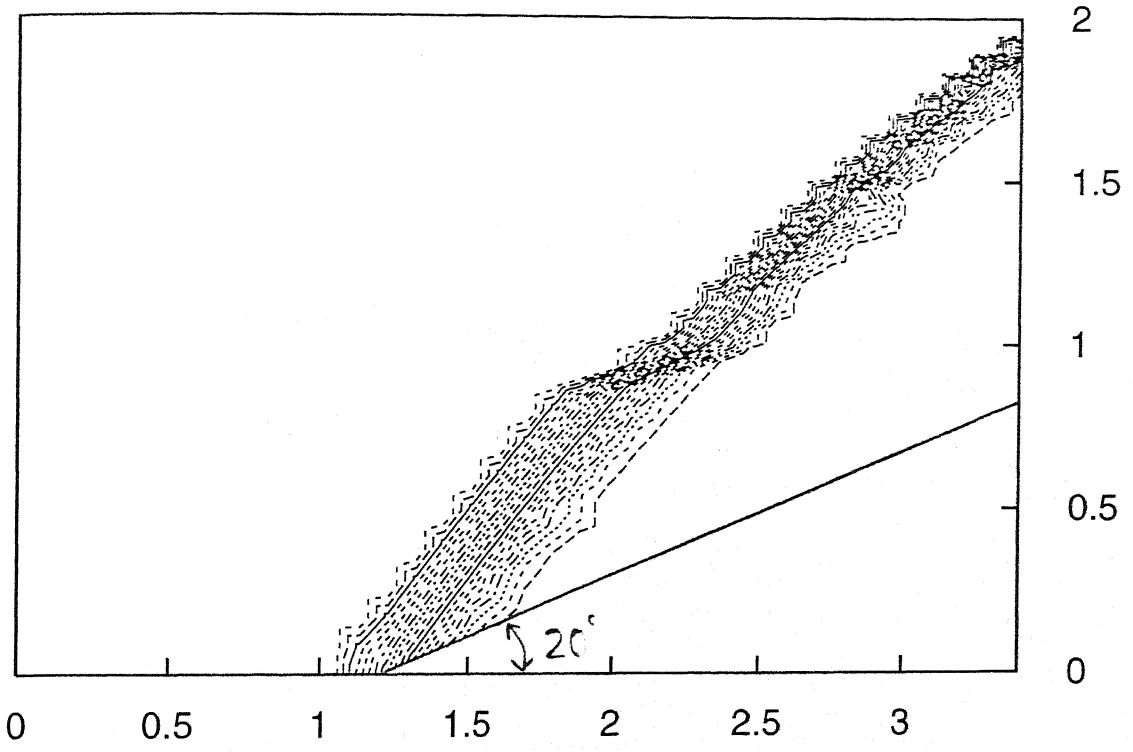

Fig. 2. Isobars for Mach 3 flow over a 20° ramp

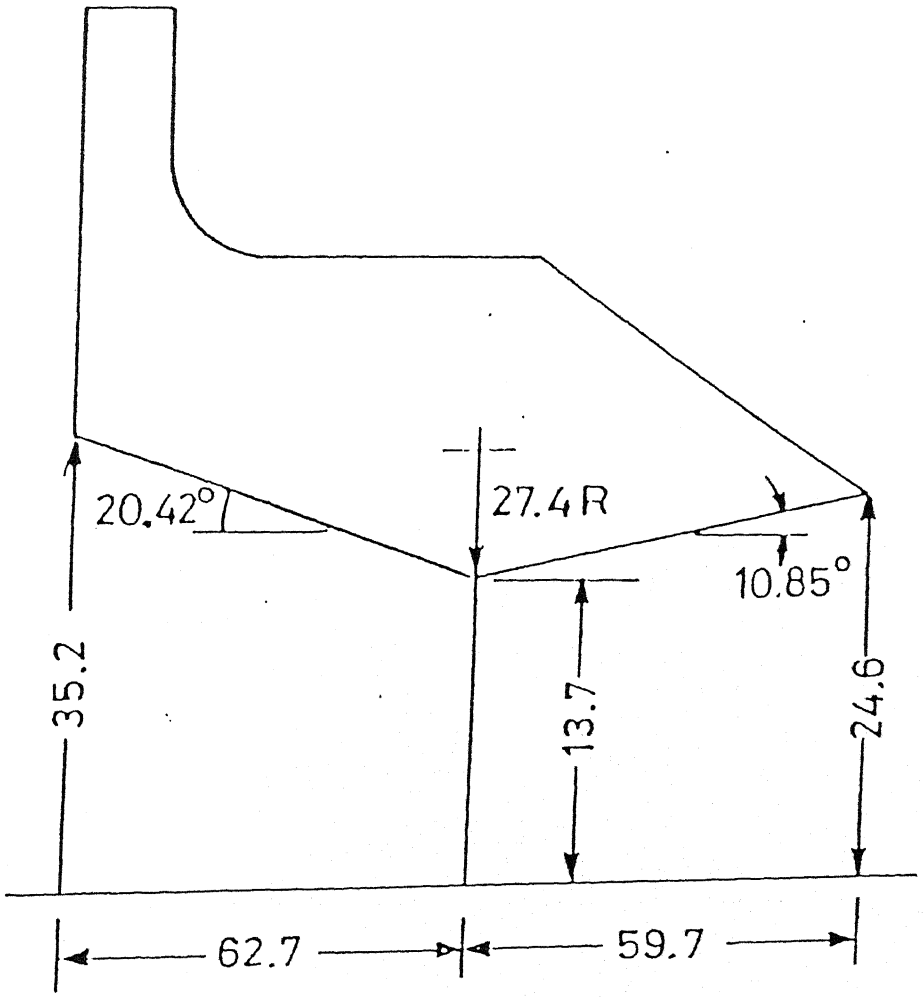

Fig. 3. 2D convergent-divergent (B3) nozzle geometry

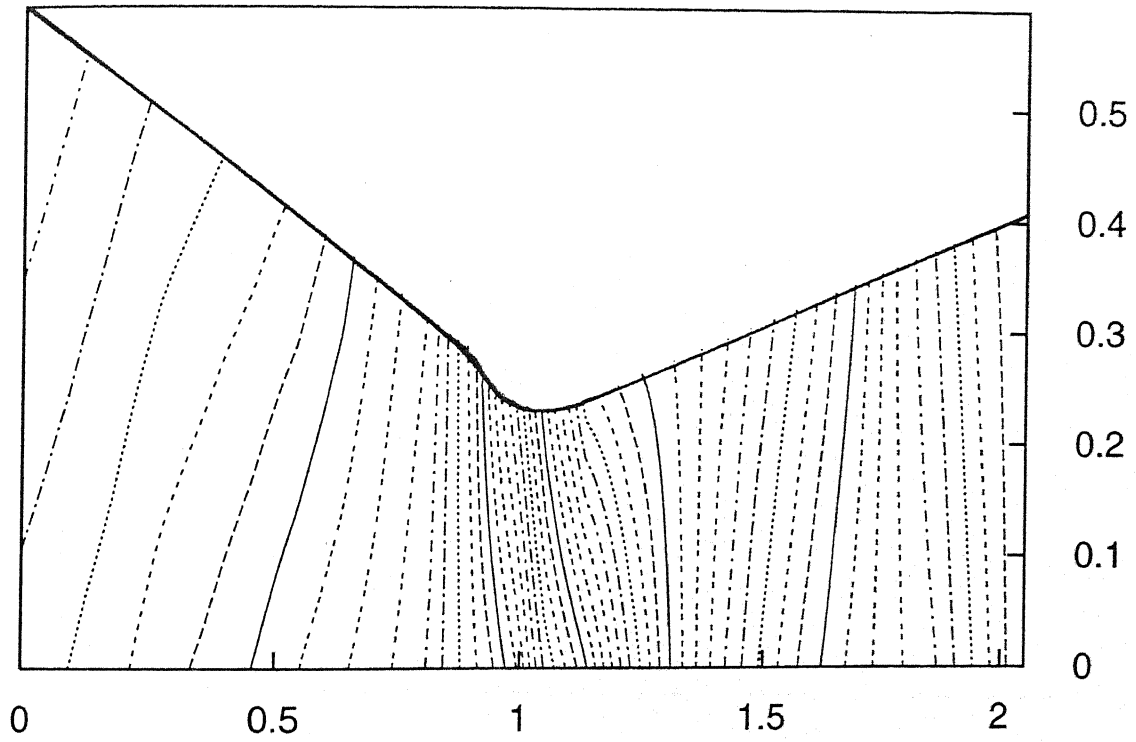

Fig. 4. Iso-Machs for B3 nozzle (P_o/p=9.0)

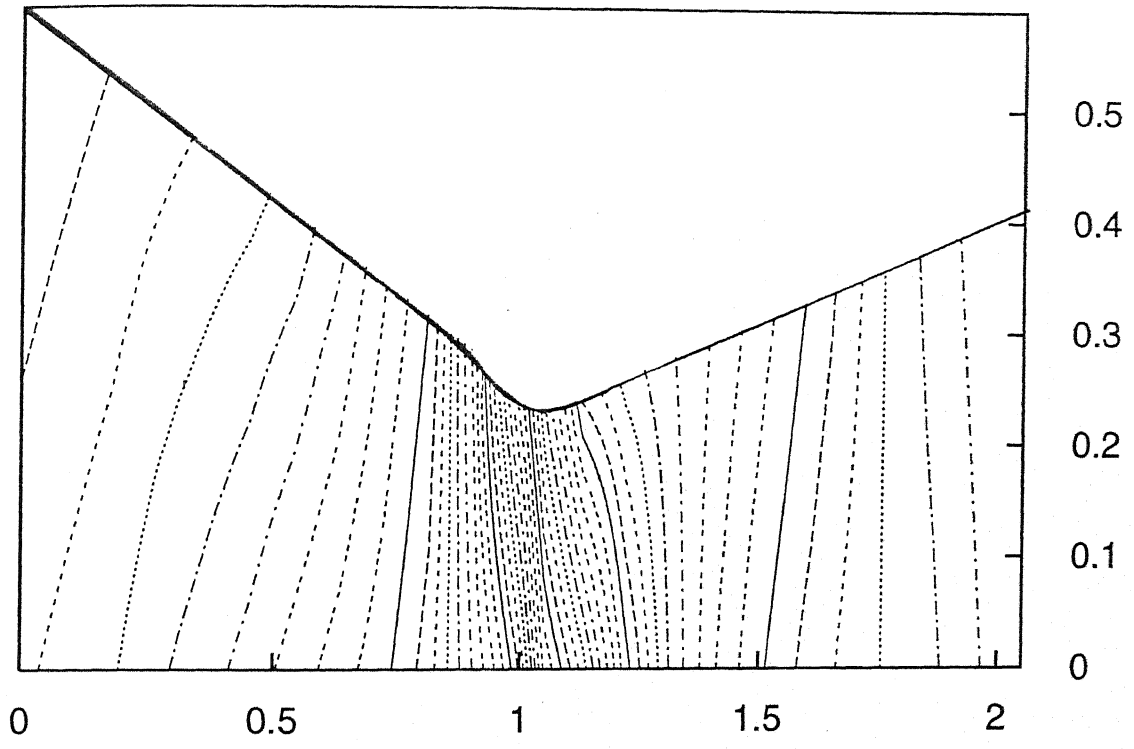

Fig. 5. Iso-bars for B3 nozzle (P_o/p=9.0)

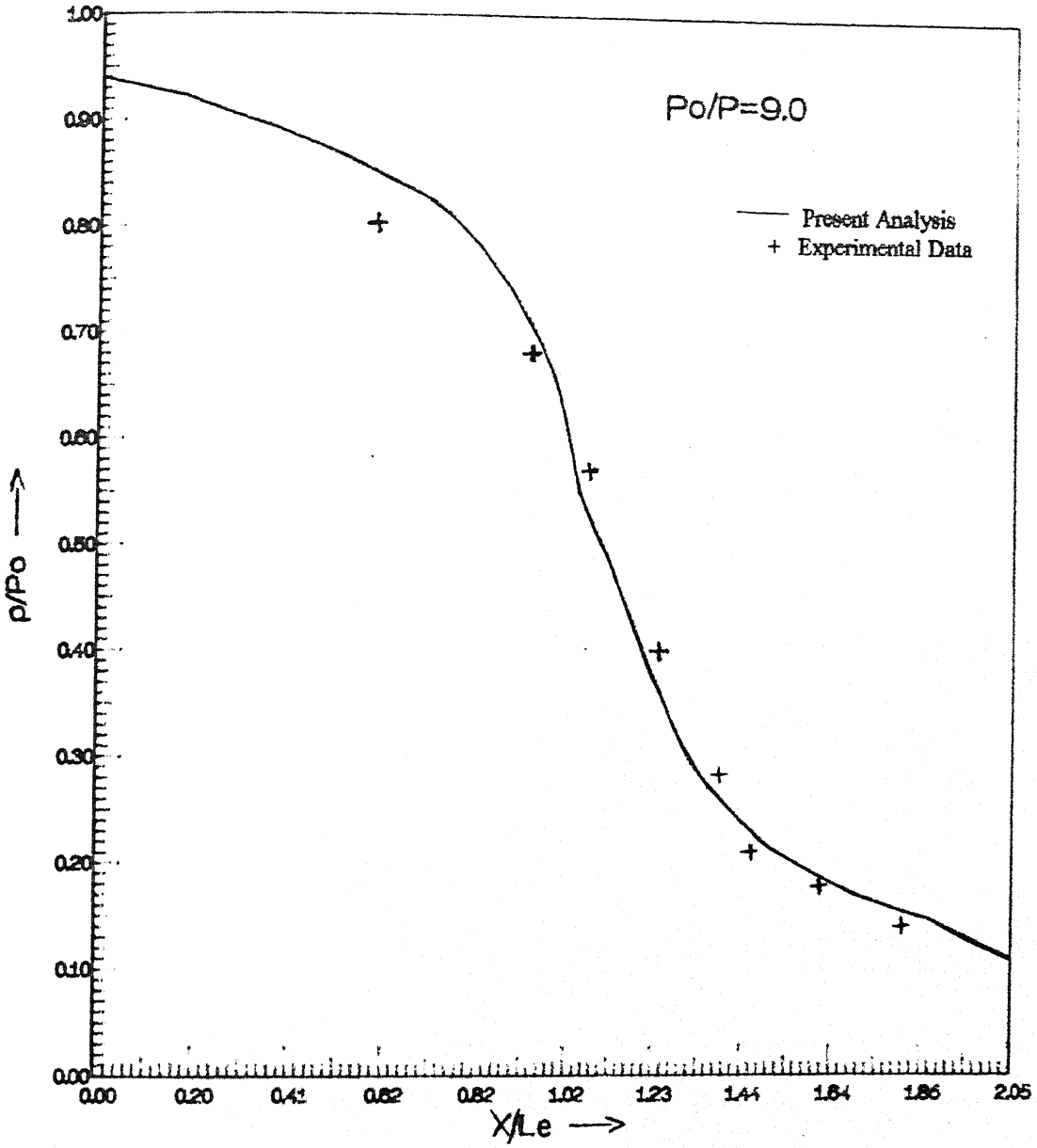

Fig. 6. Centre-line Pressure distribution for B3 nozzle (P_o/p=9.0)

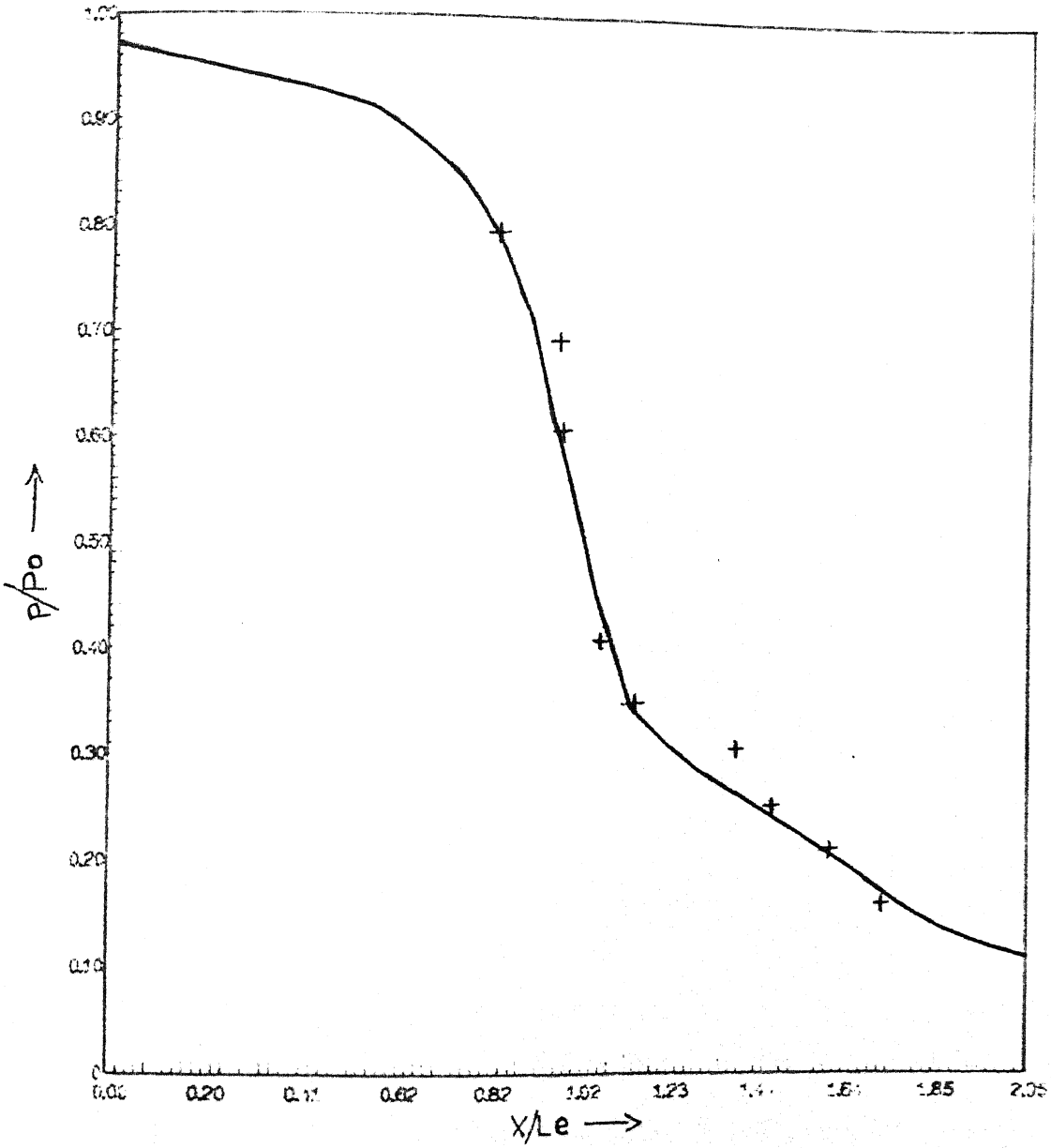

Fig. 7. Wall Pressure distribution for B3 nozzle (P_o/p=9.0)

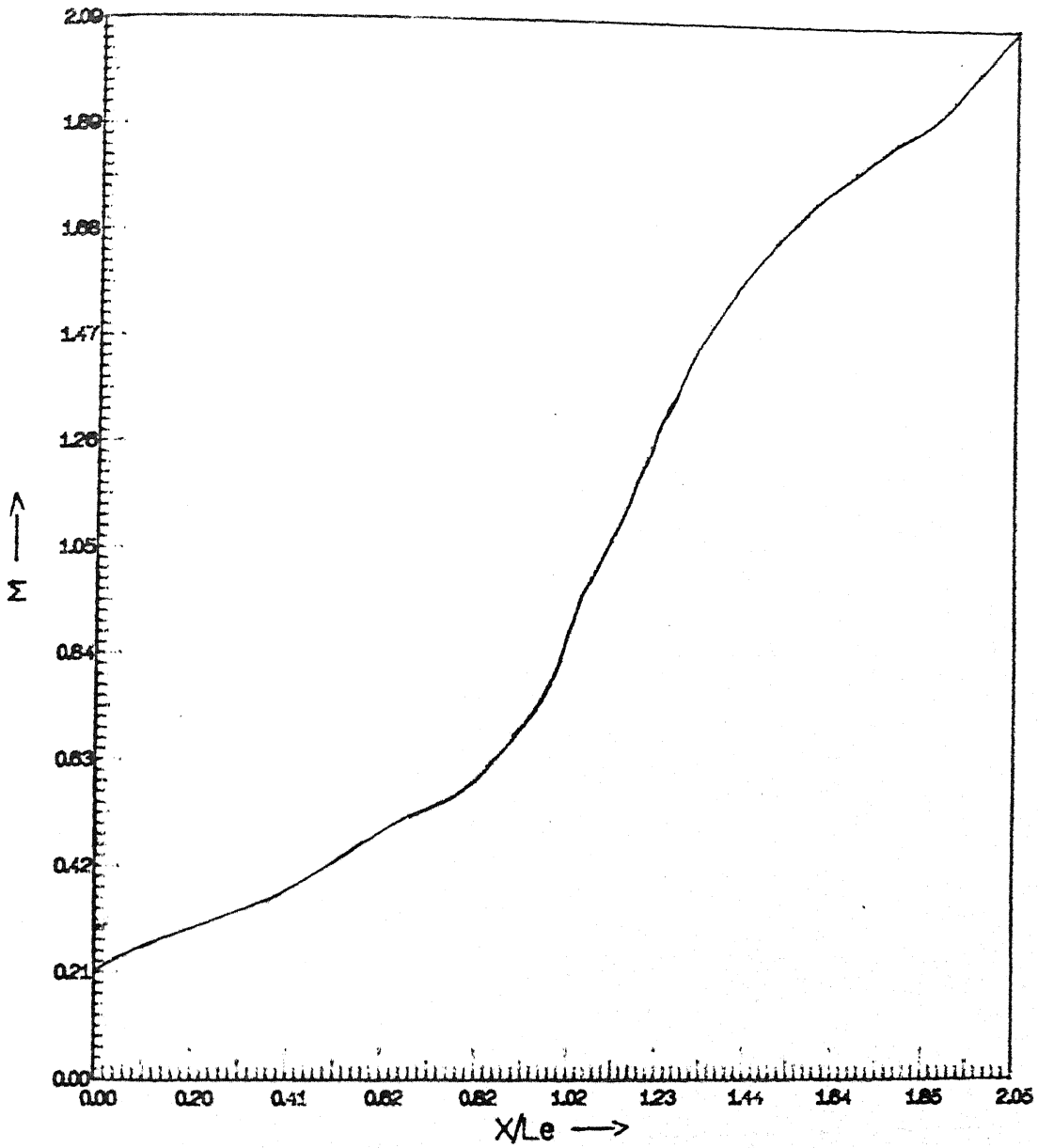

Fig. 8. Centre-line Mach no. distribution for B3 nozzle ($P_o/p=9.0$)

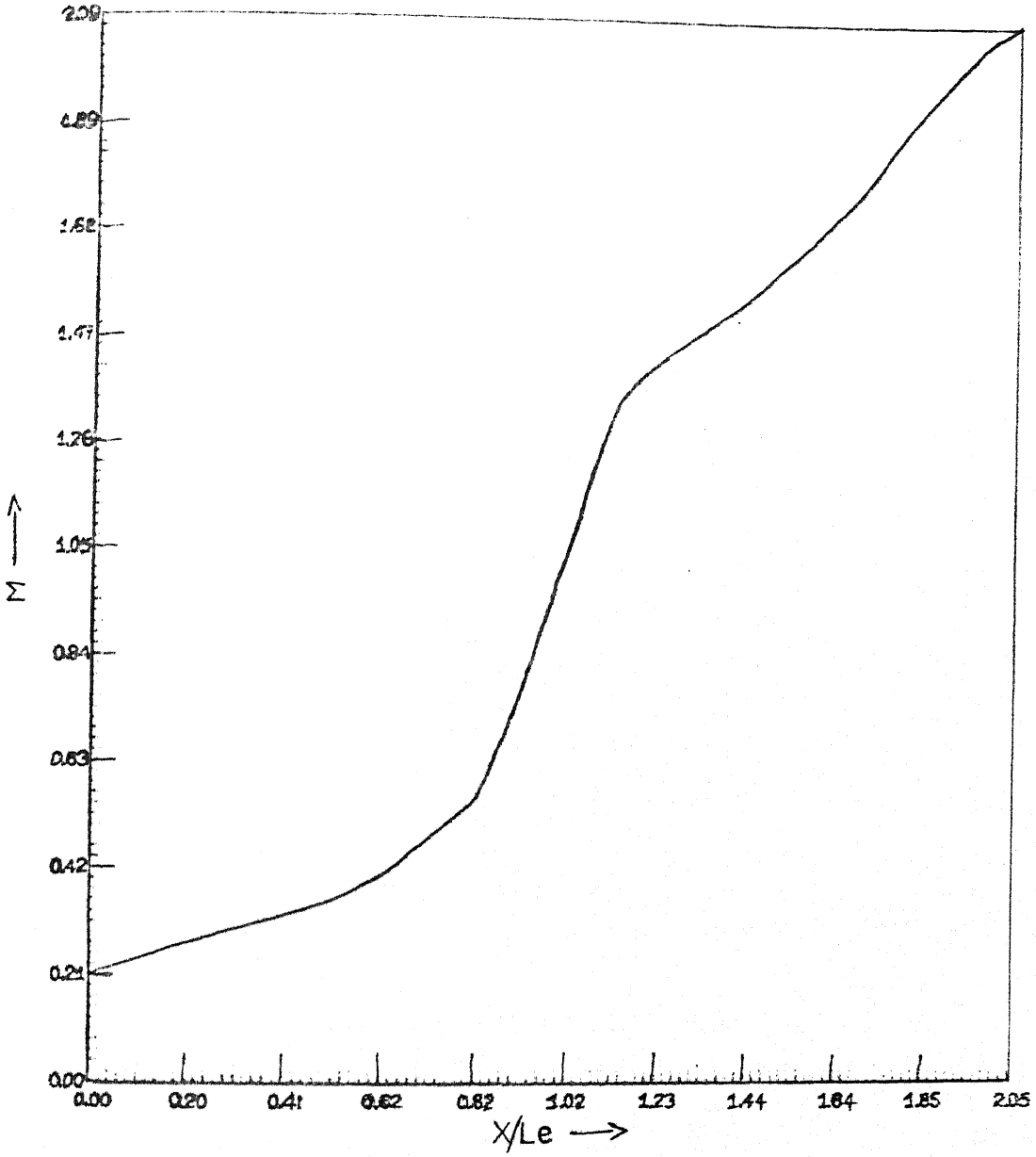

Fig. 9. Wall Mach No. distribution for B3 nozzle (P_o/p=9.0)

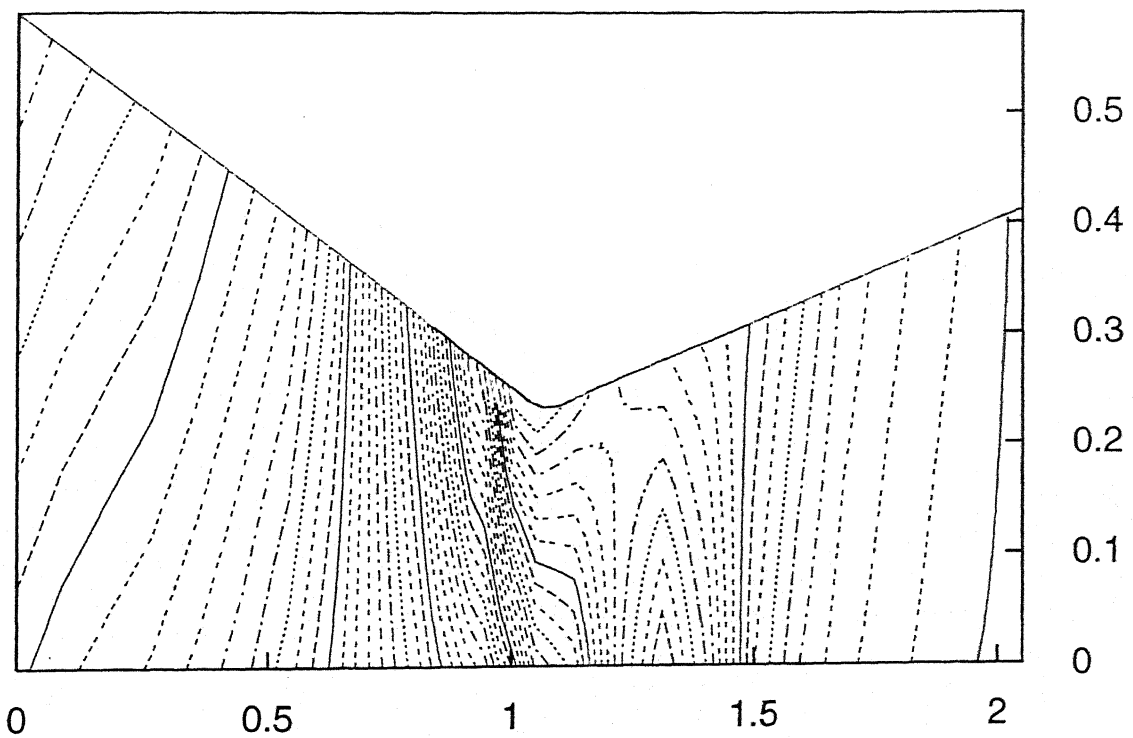

Fig. 10. Iso-Machs for B3 nozzle (P_o/p=1.98)

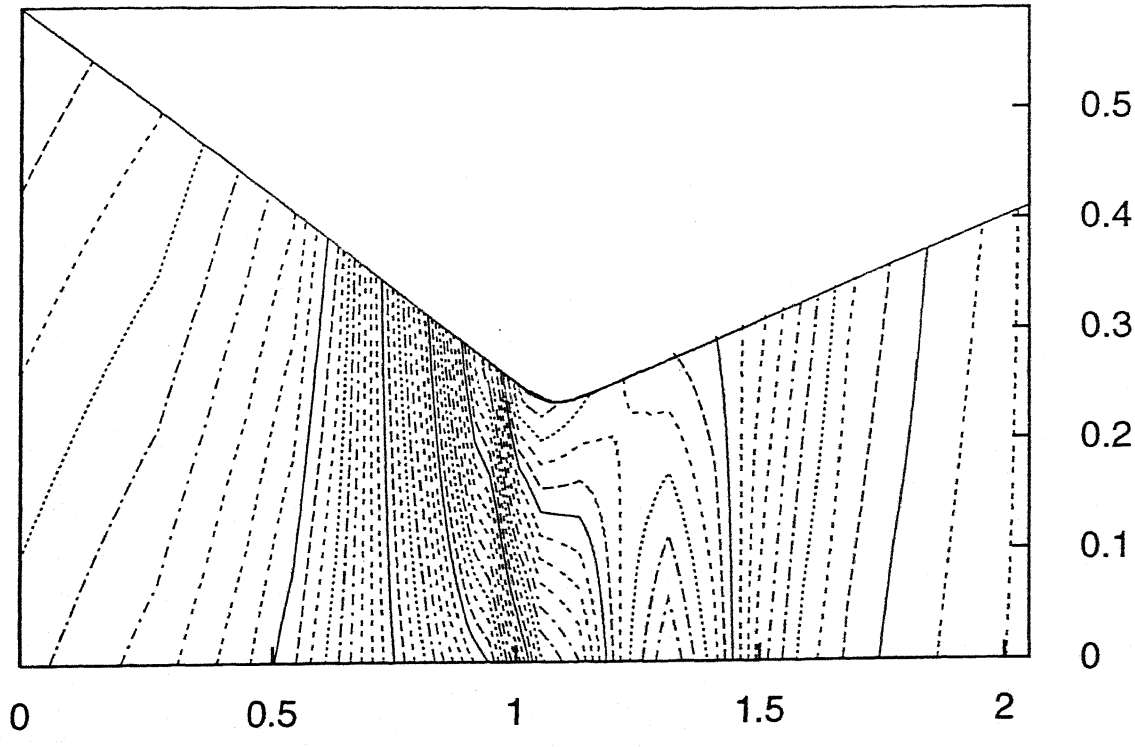

Fig. 11. Iso-bars for B3 nozzle (P_o/p=1.98)

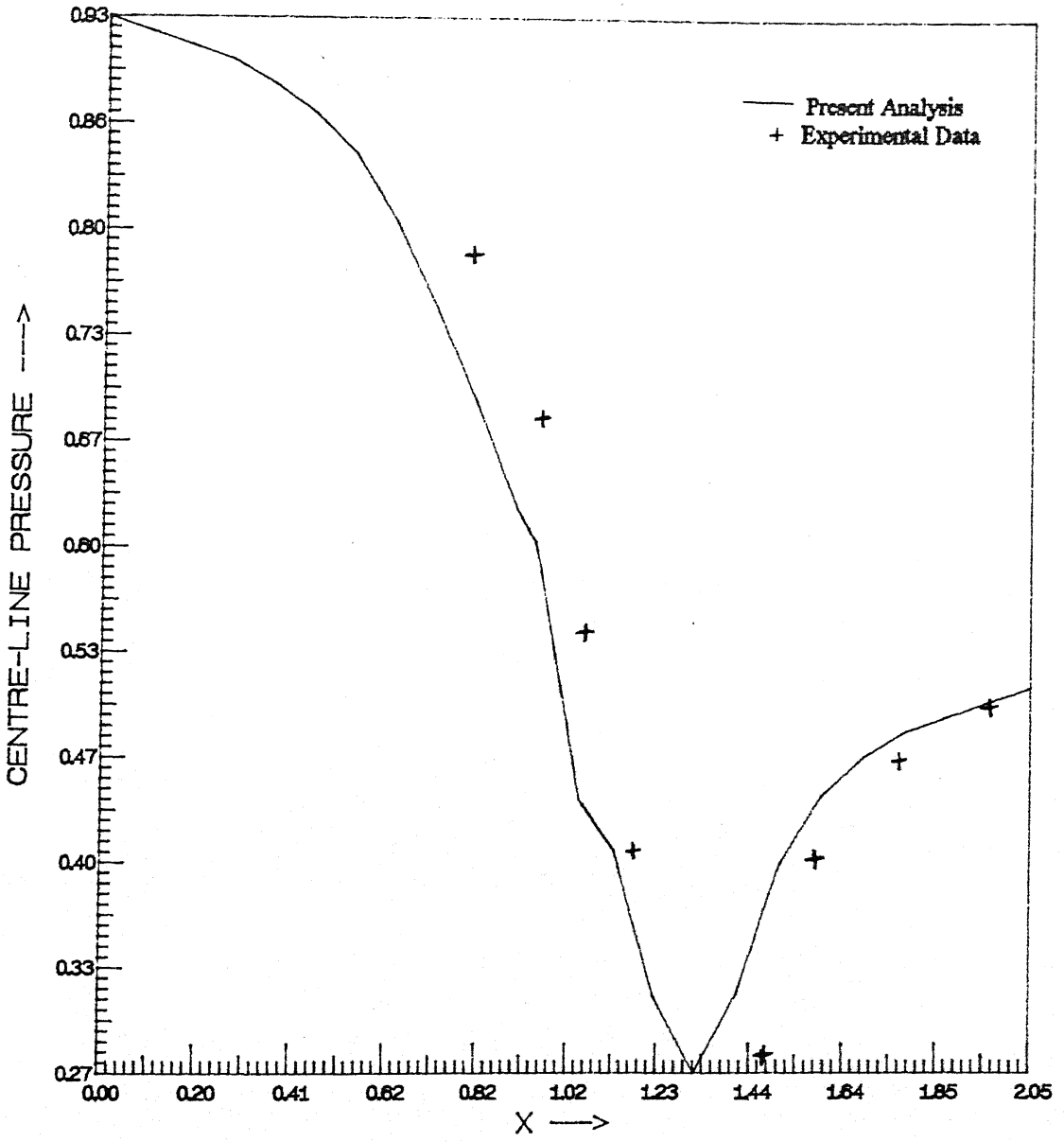

Fig. 12. Centre-line Pressure distribution for B3 nozzle (P_o/p=1.98)

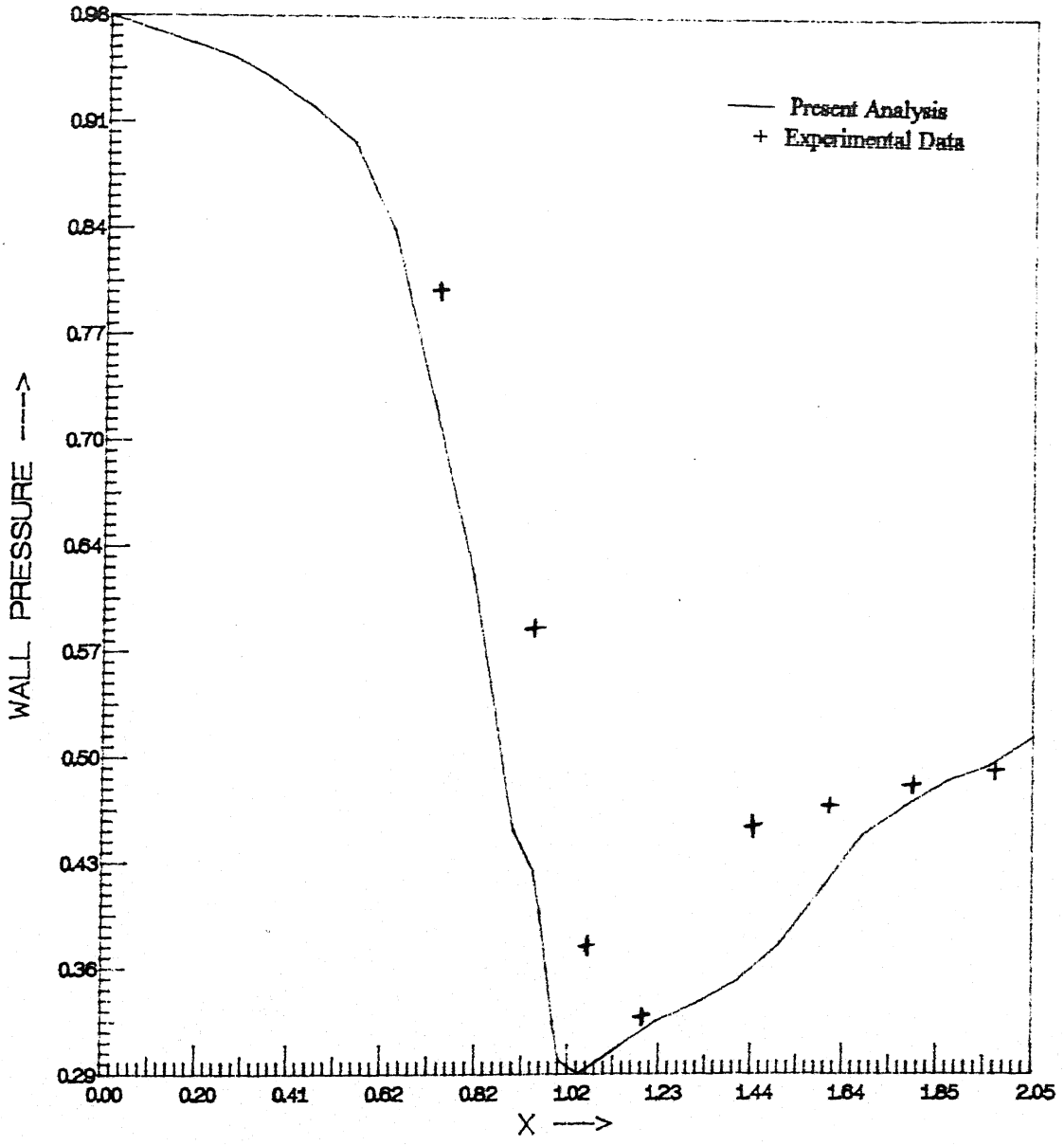

Fig. 13. Wall Pressure distribution for B3 nozzle (P_o/p=1.98)

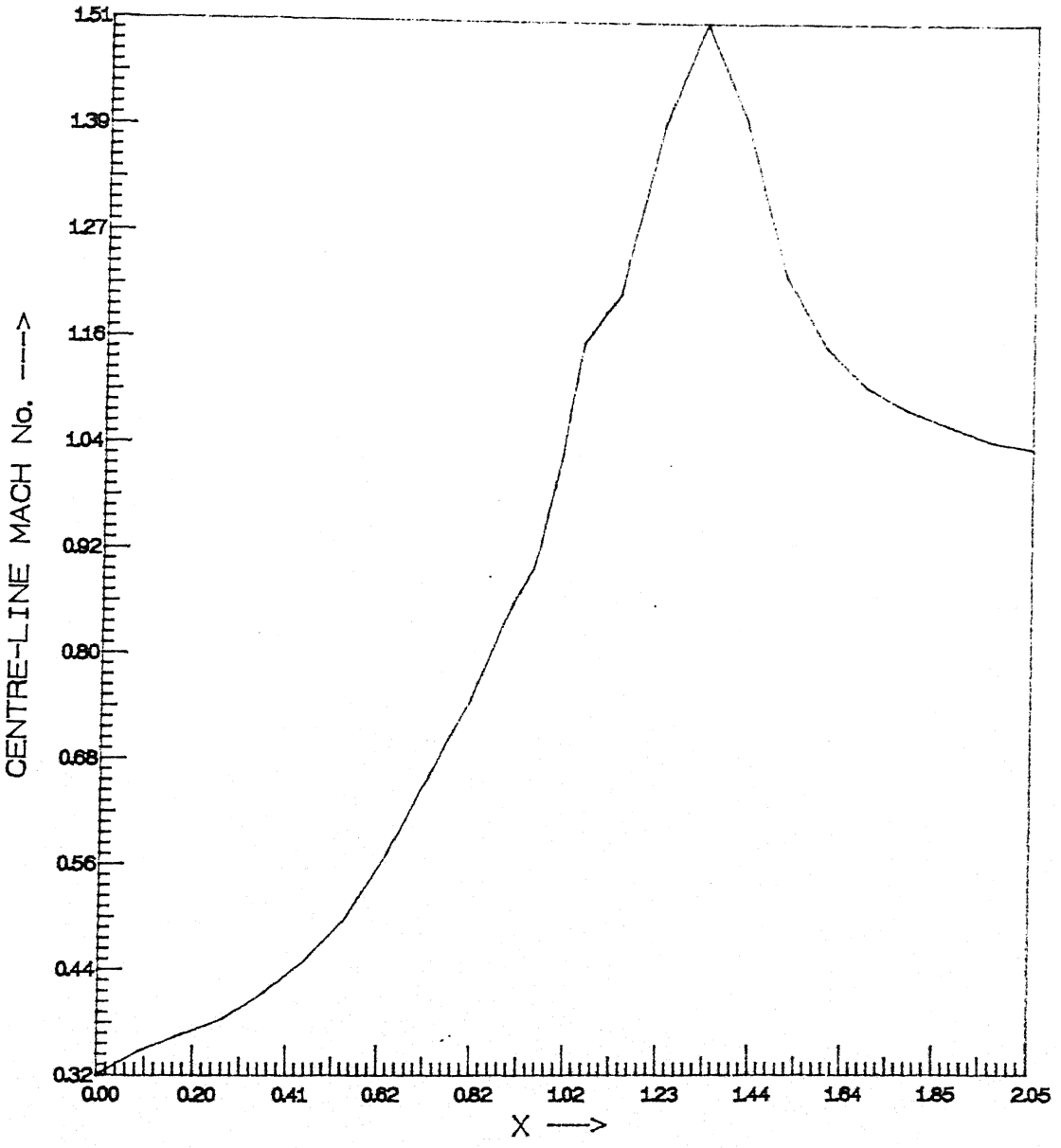

Fig. 14. Centre-line Mach No. distribution for B3 nozzle (P_o/p=1.98)

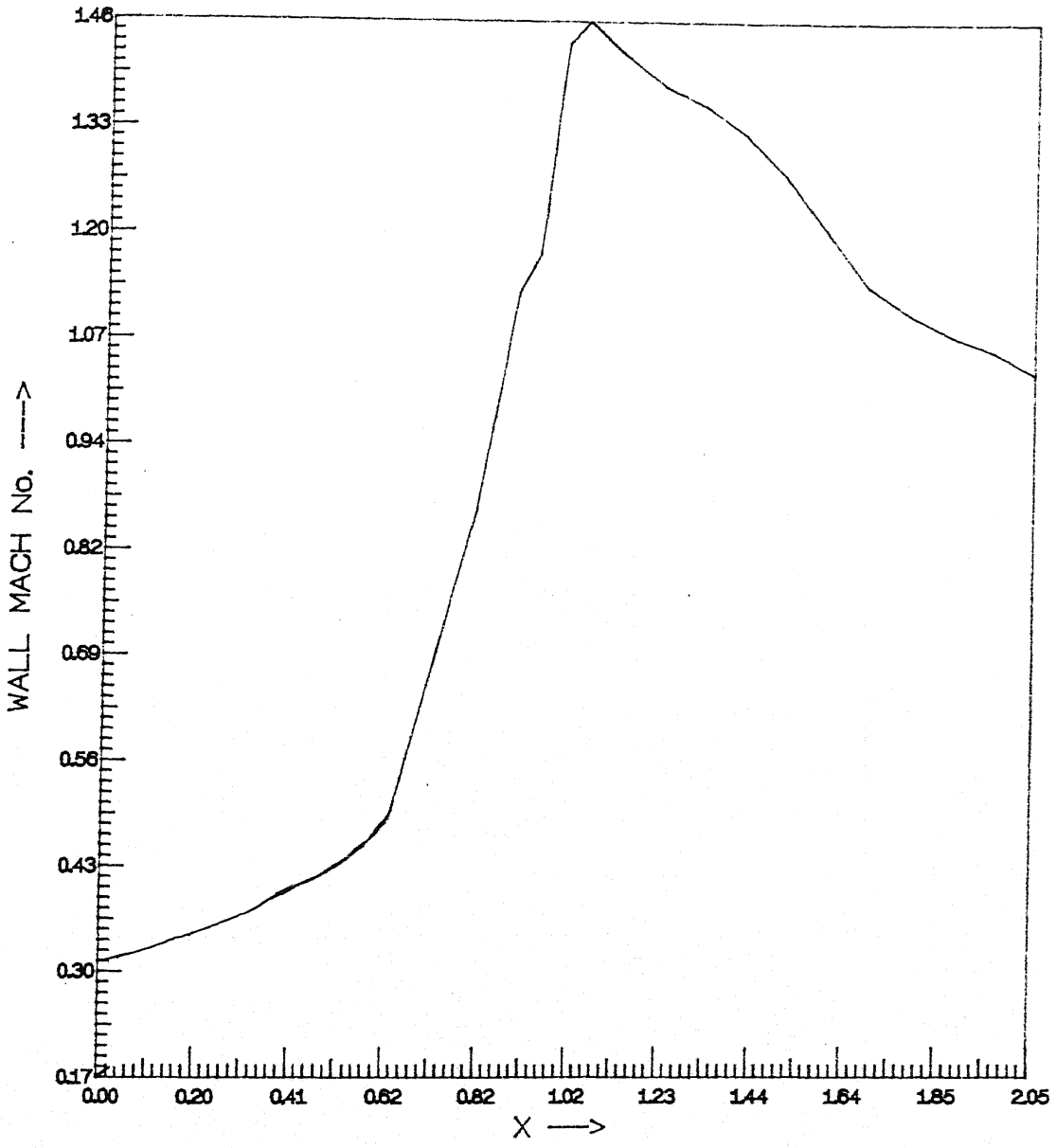

Fig. 15. Wall Mach No. distribution for B3 nozzle (P_o/p=1.98)

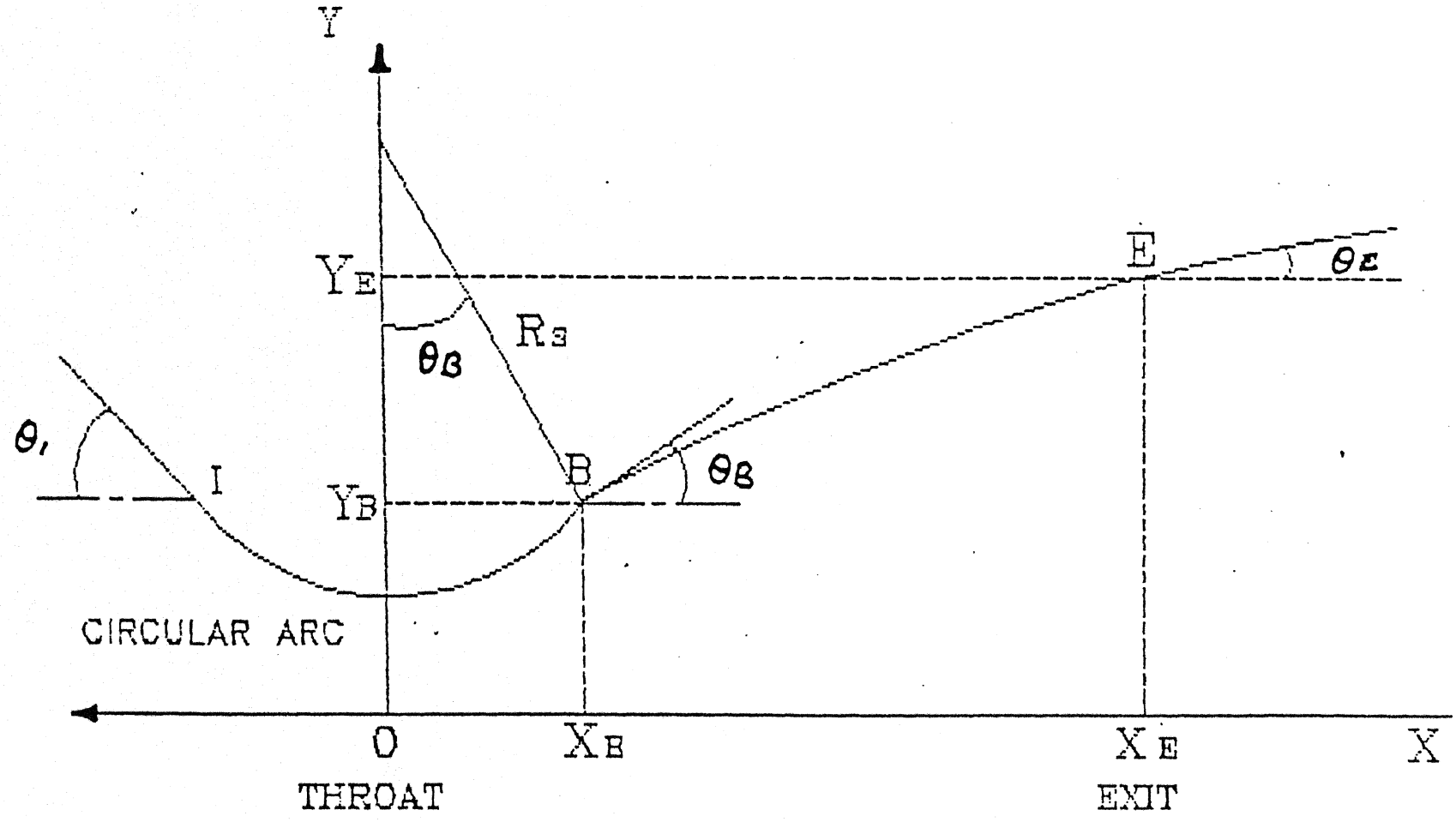

Fig. 16. Axisymmetric nozzle geometry

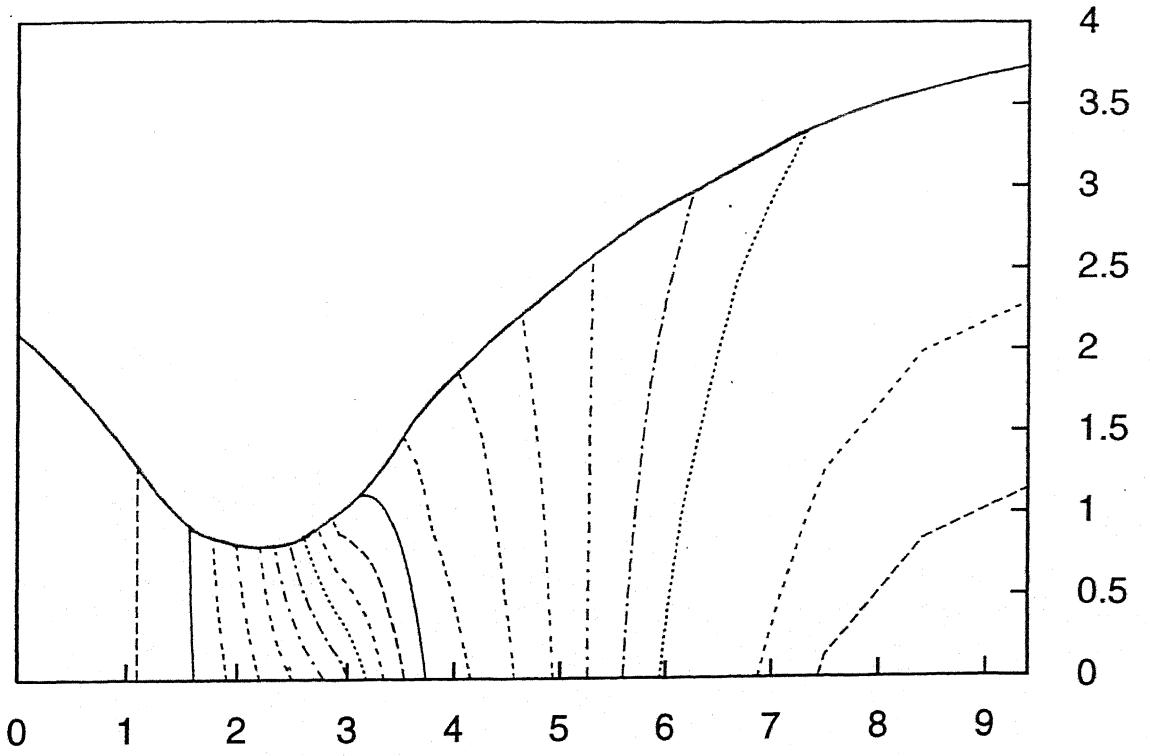

Fig. 17. Iso-machs for axisymmetric nozzle

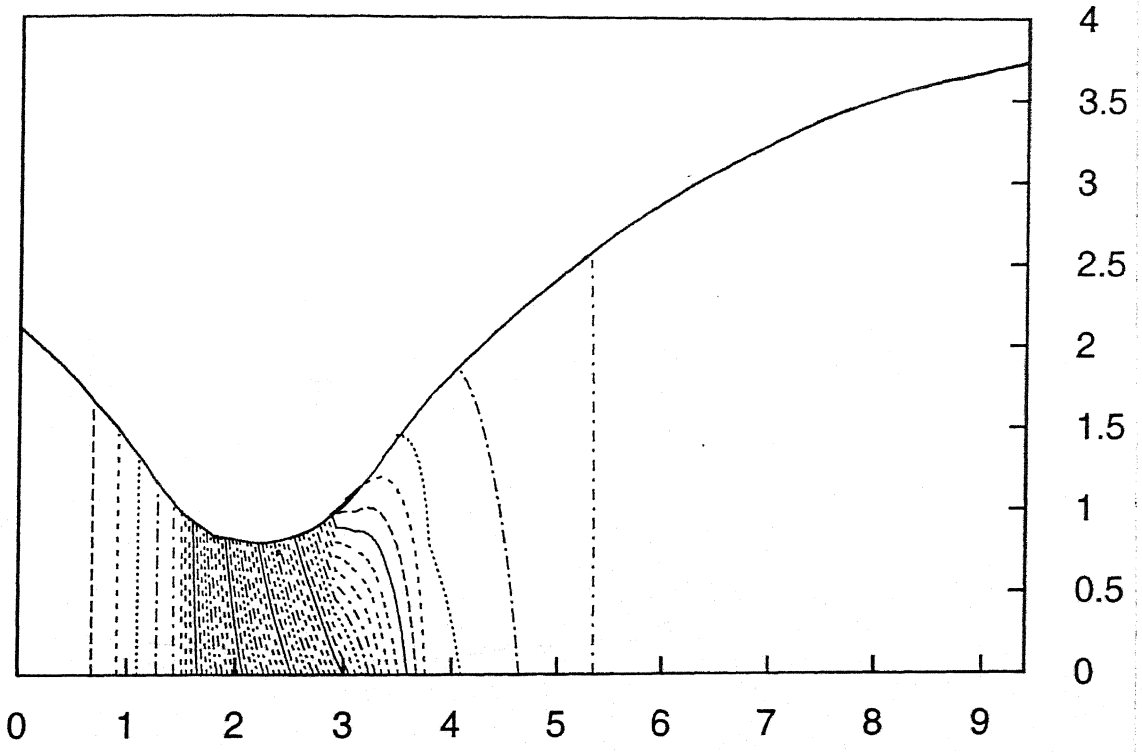

Fig. 18. Iso-bars for axisymmetric nozzle

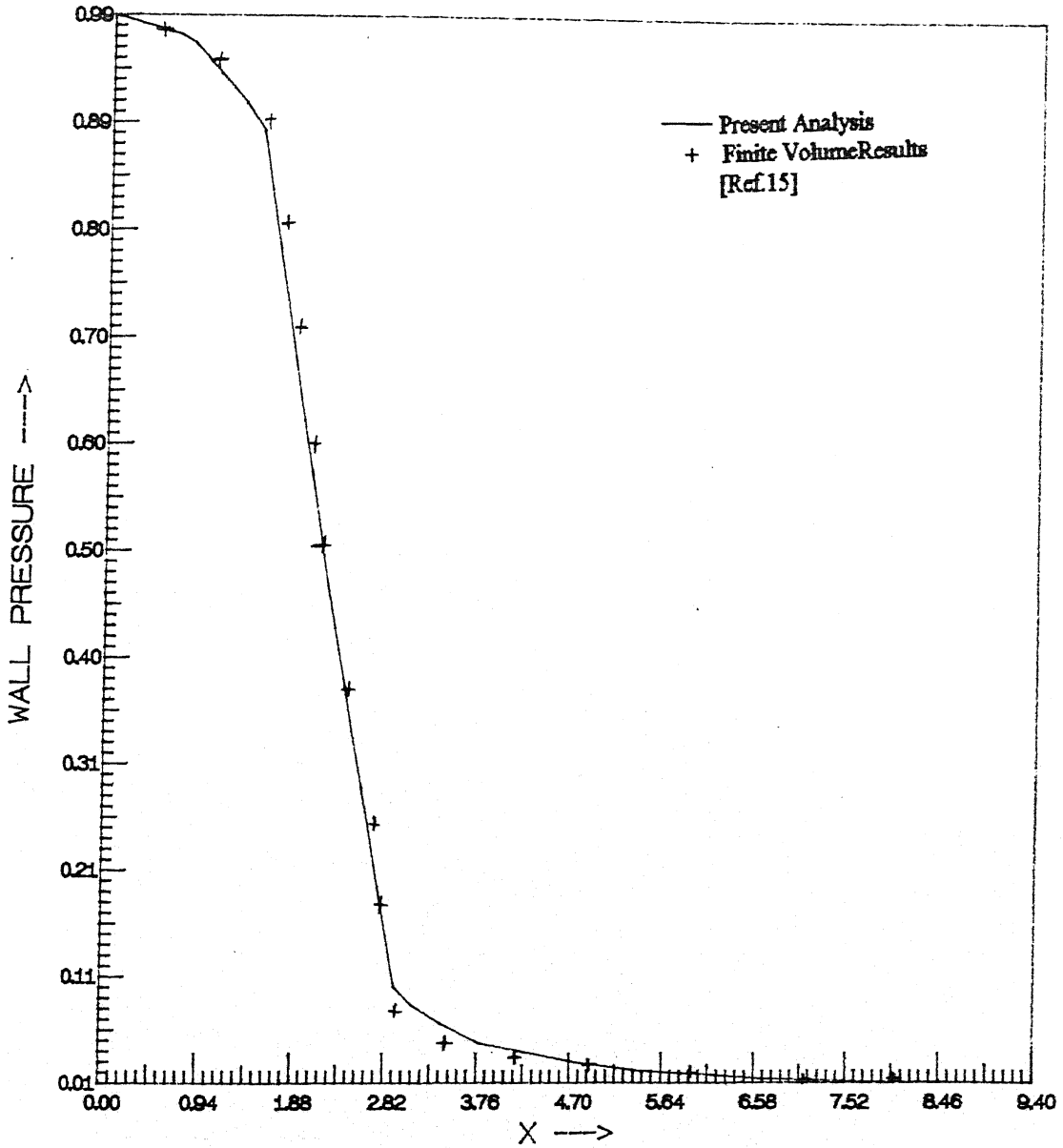

Fig. 19. Wall Pressure distribution for Axisymmetric nozzle

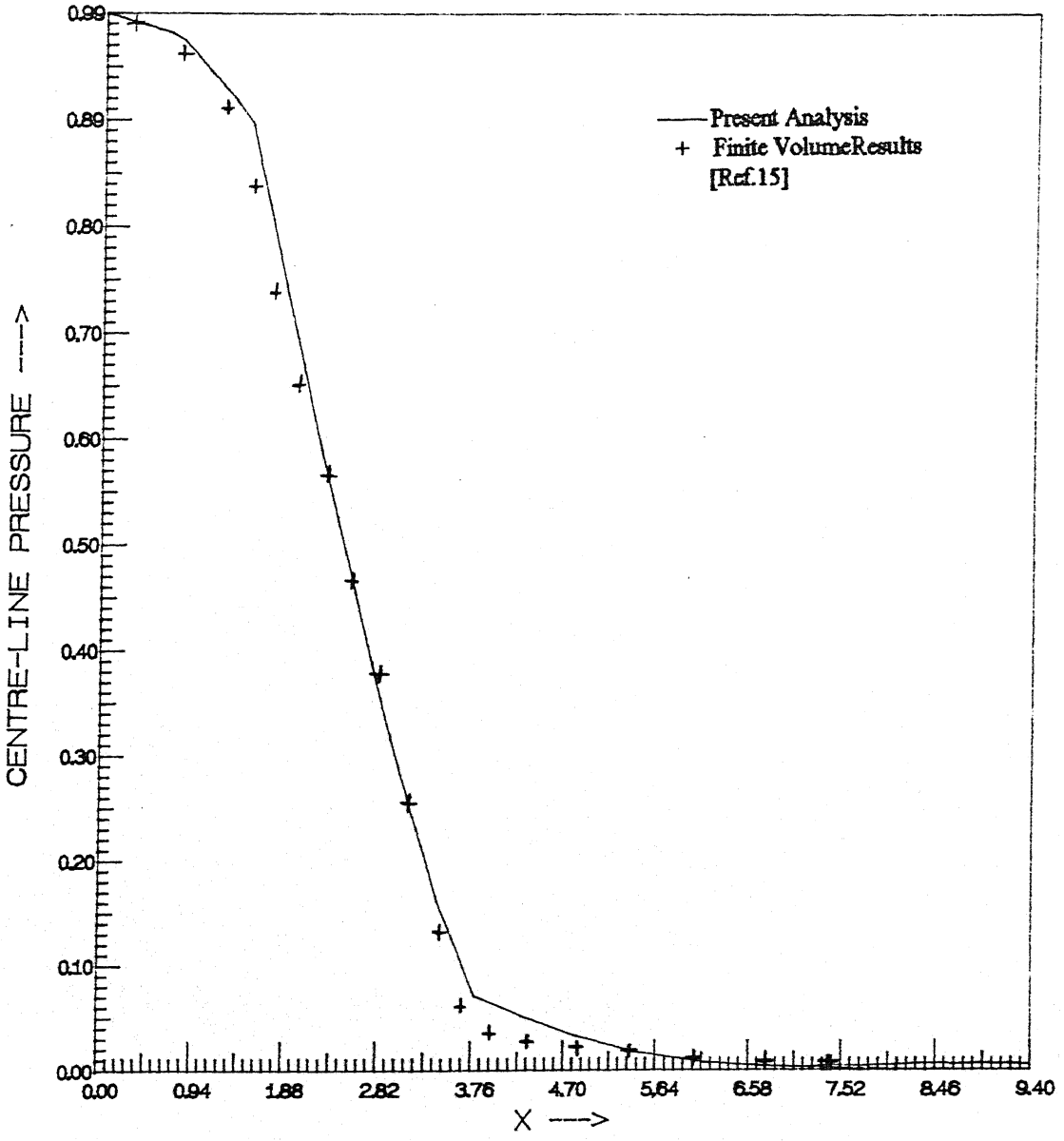

Fig. 20. Centre-line Pressure distribution for Axisymmetric nozzle

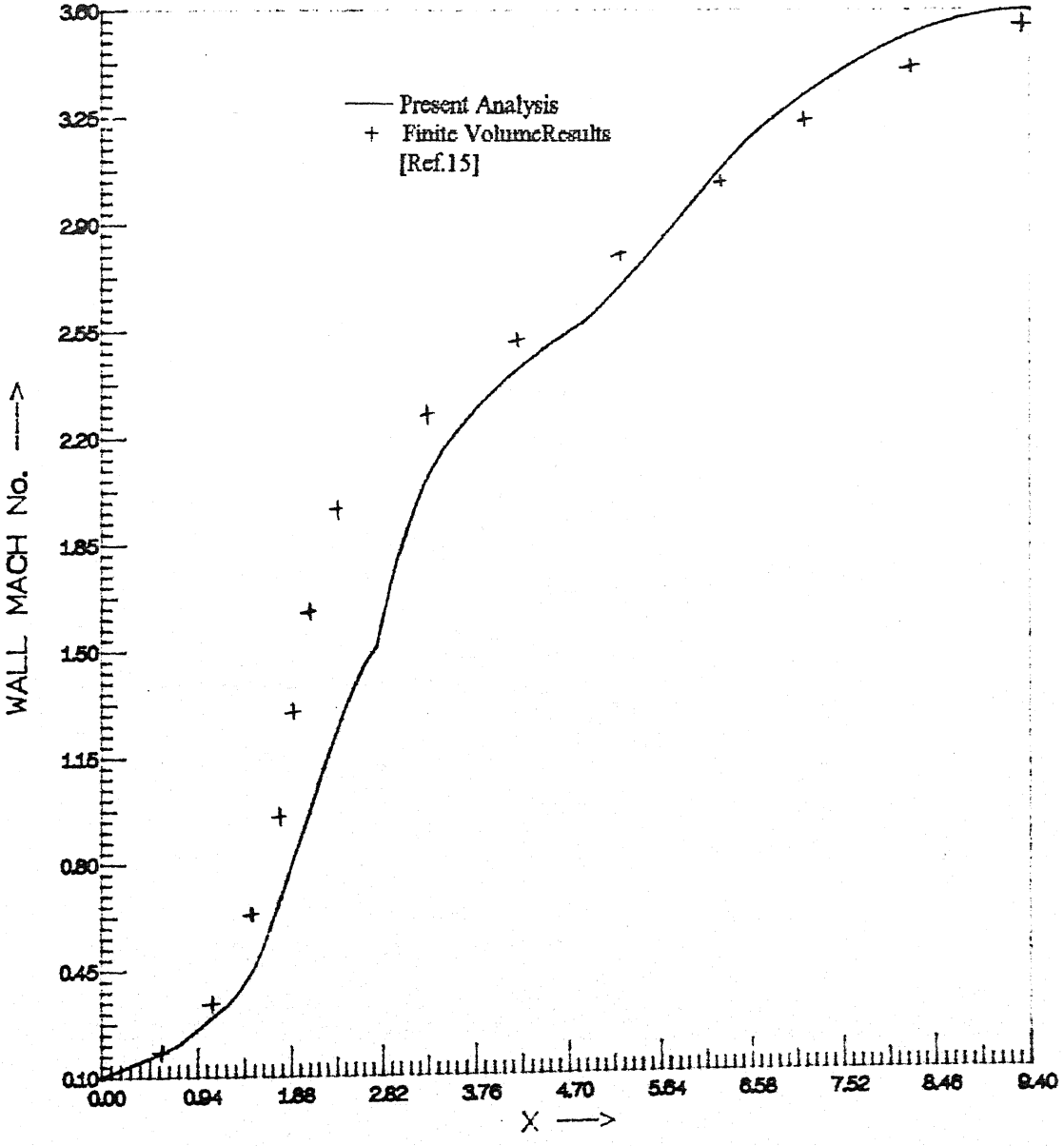

Fig. 21. Wall Mach No. distribution for Axisymmetric nozzle

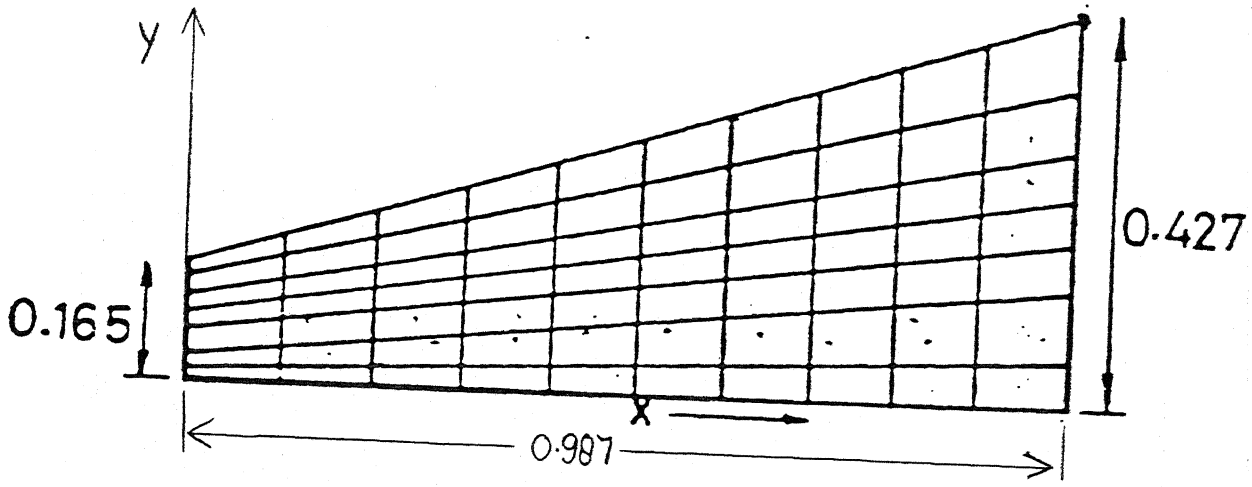

Fig. 23. 2D nozzle (half angle 15°) geometry

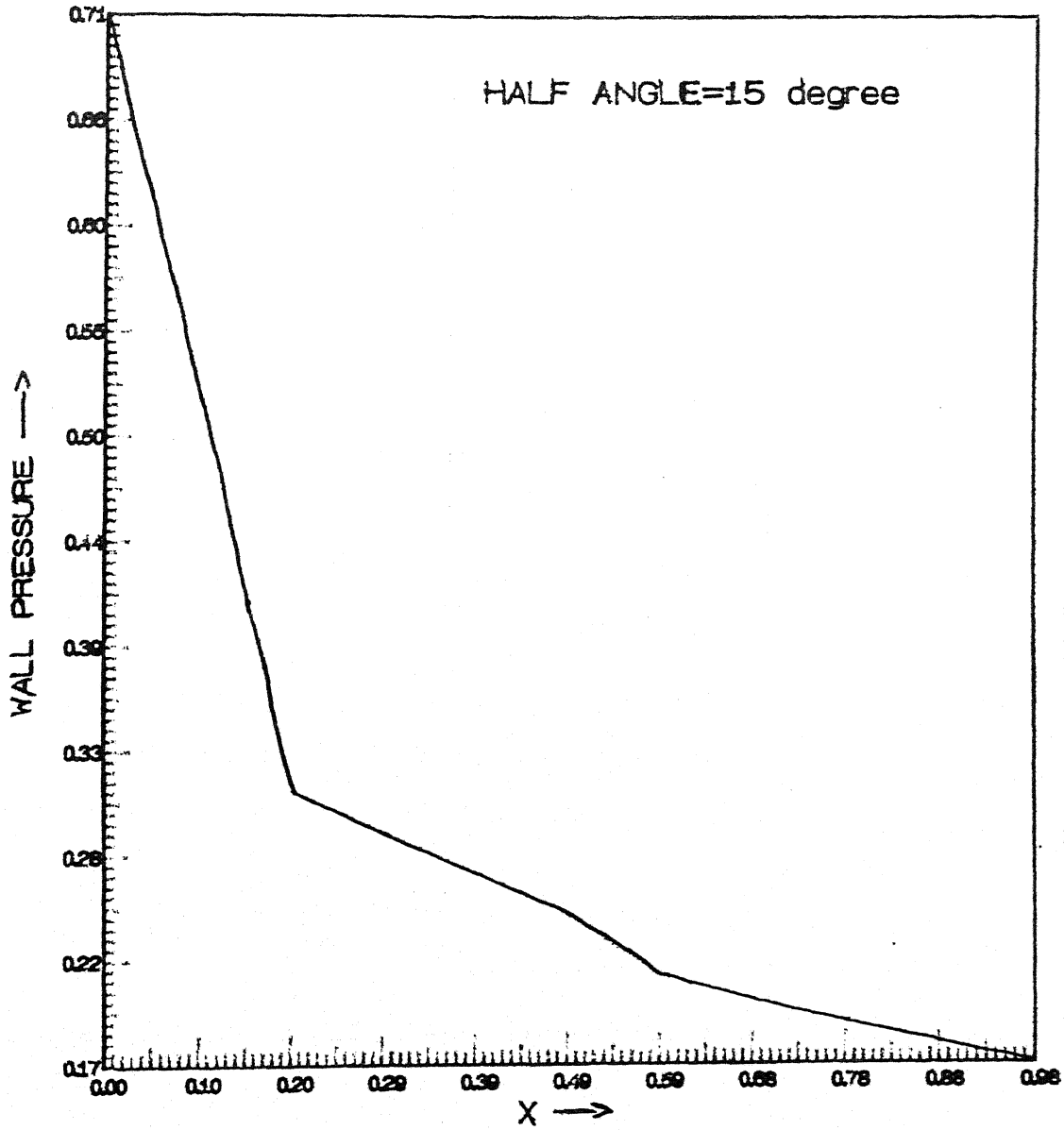

Fig. 24. Wall Pressure distribution for 2D nozzle (half angle 15°)

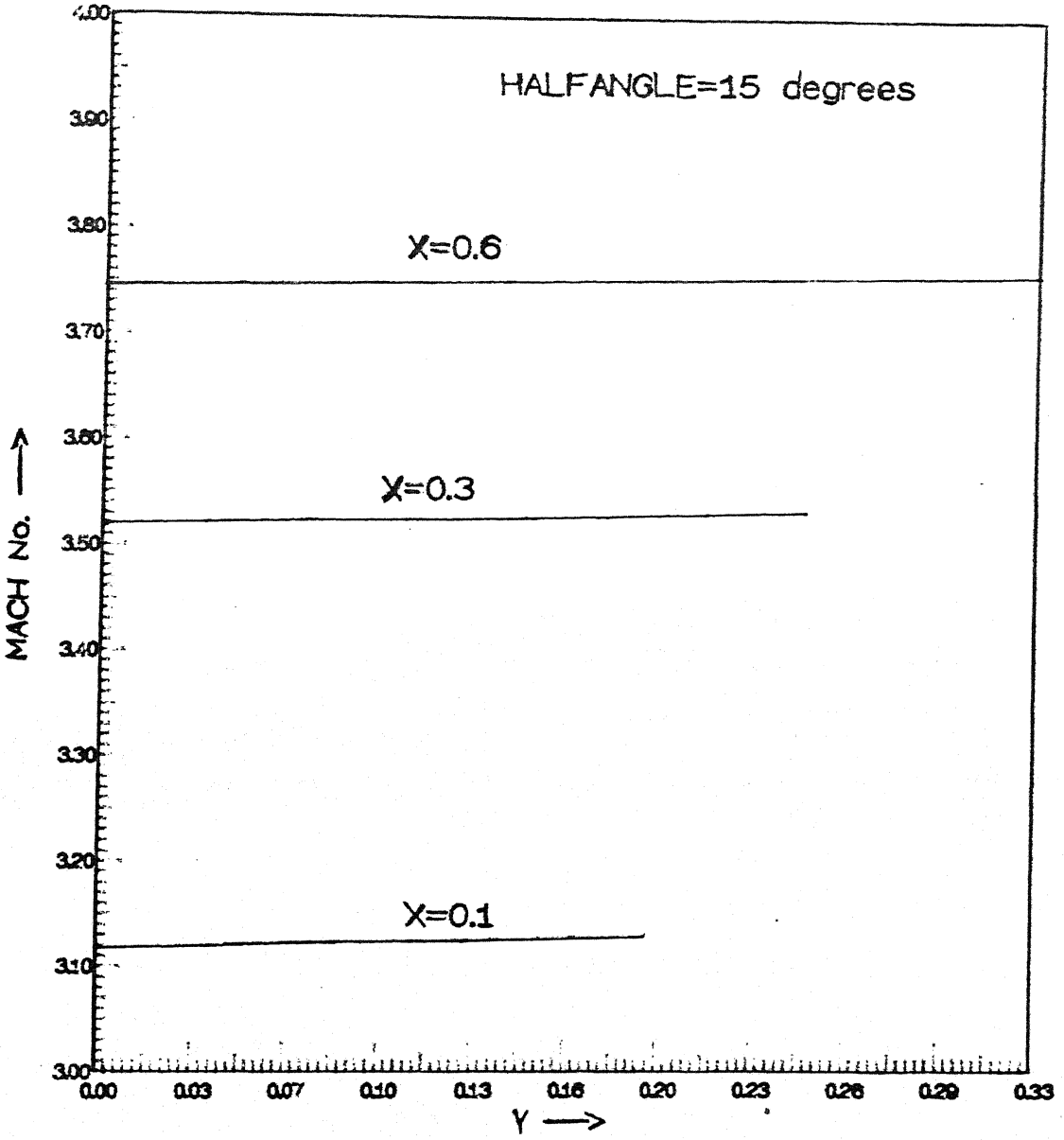

Fig. 25. Mach No. distribution at various axial stations for 2D nozzle (half angle 15°)

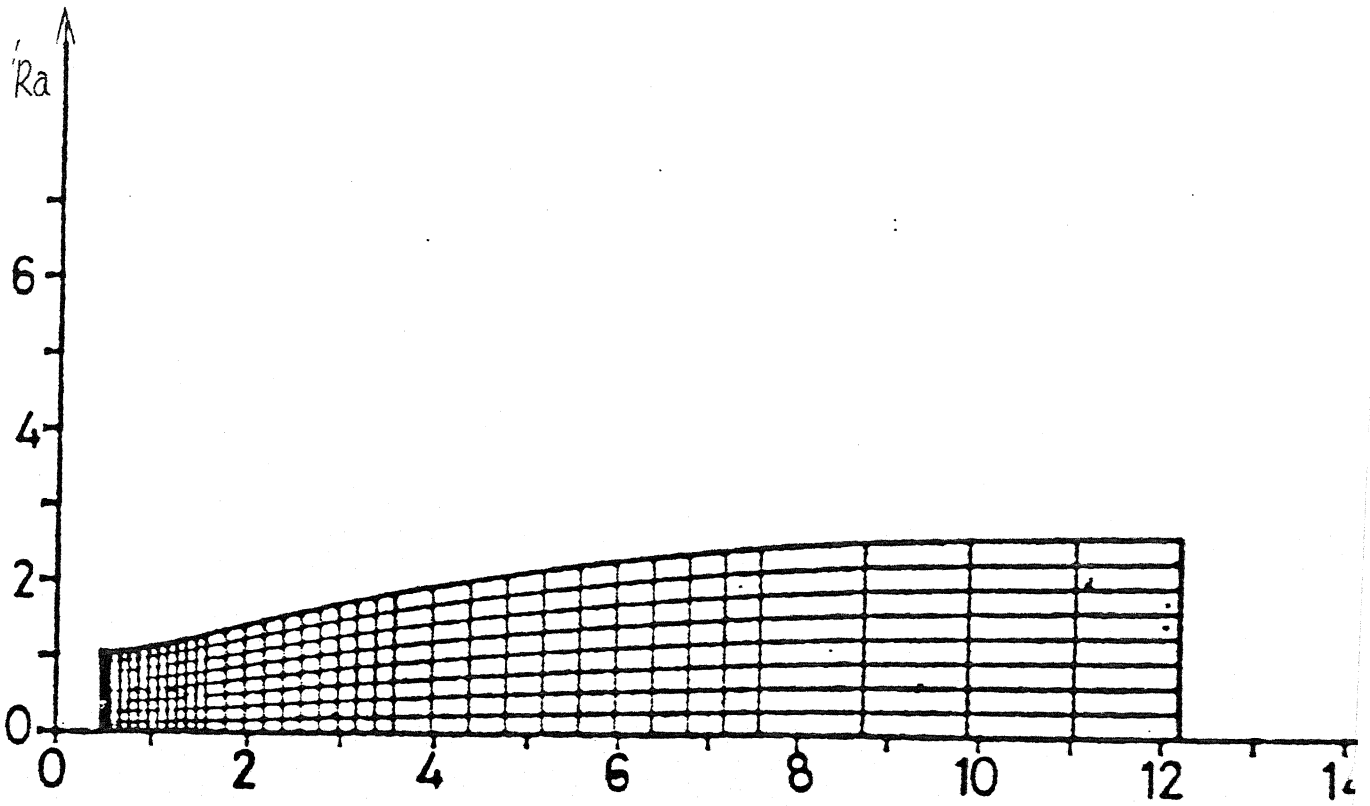

Fig. 26. TND-2579 nozzle geometry (Axisymmetric)

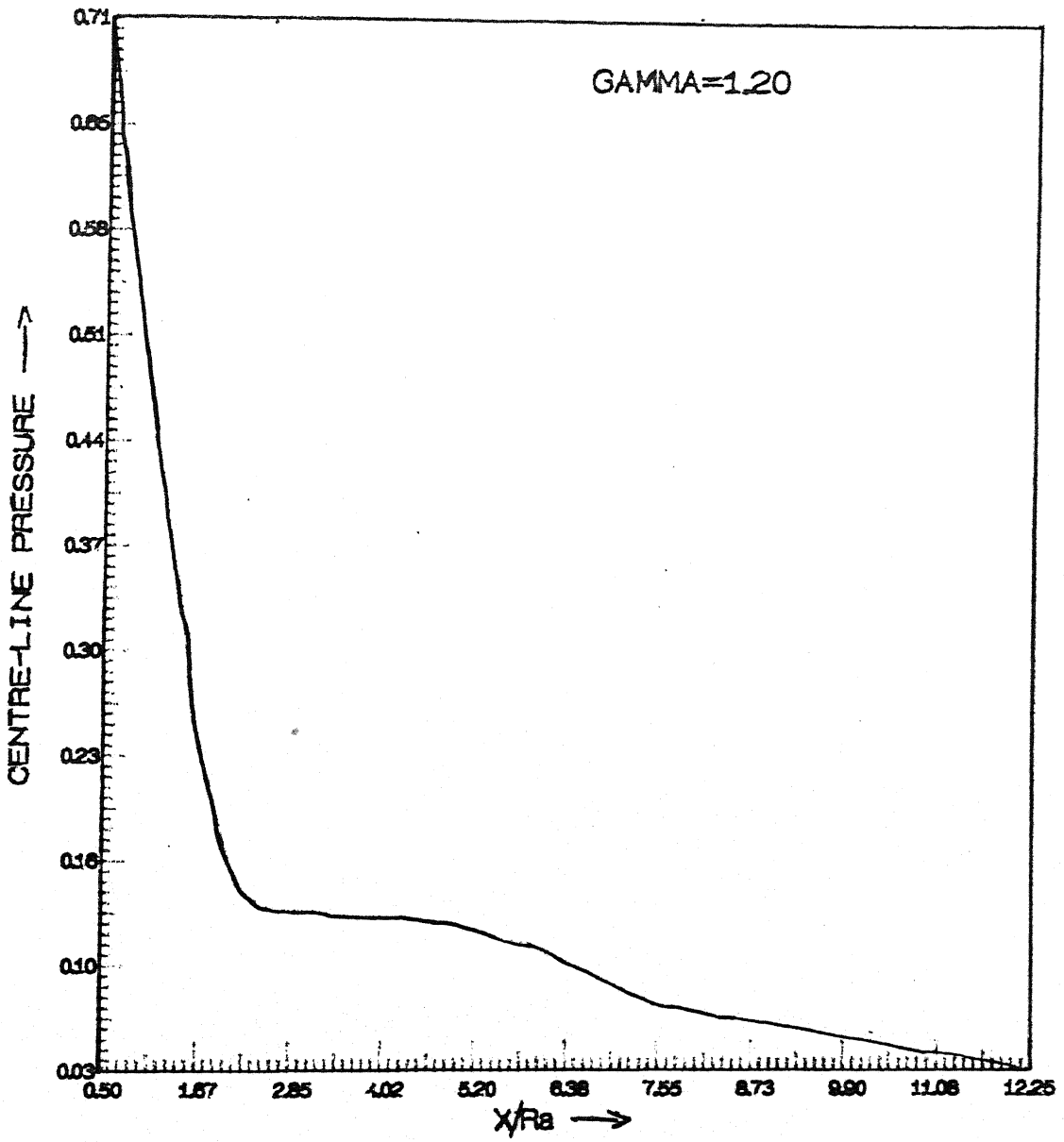

Fig. 27. Centre-line Pressure distribution for TND-2579 nozzle

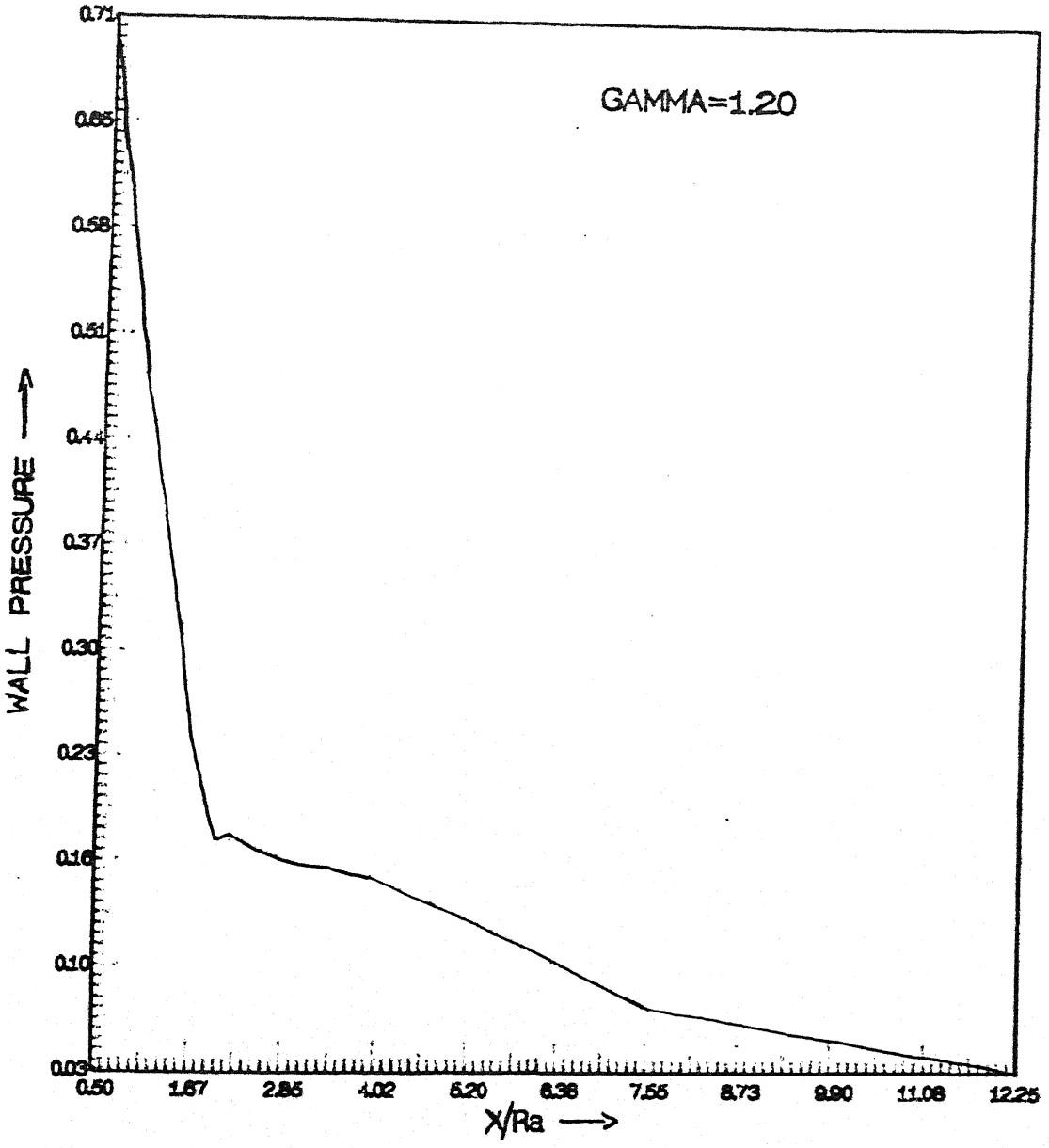

Fig. 28. Wall Pressure distribution for TND-2579 nozzle

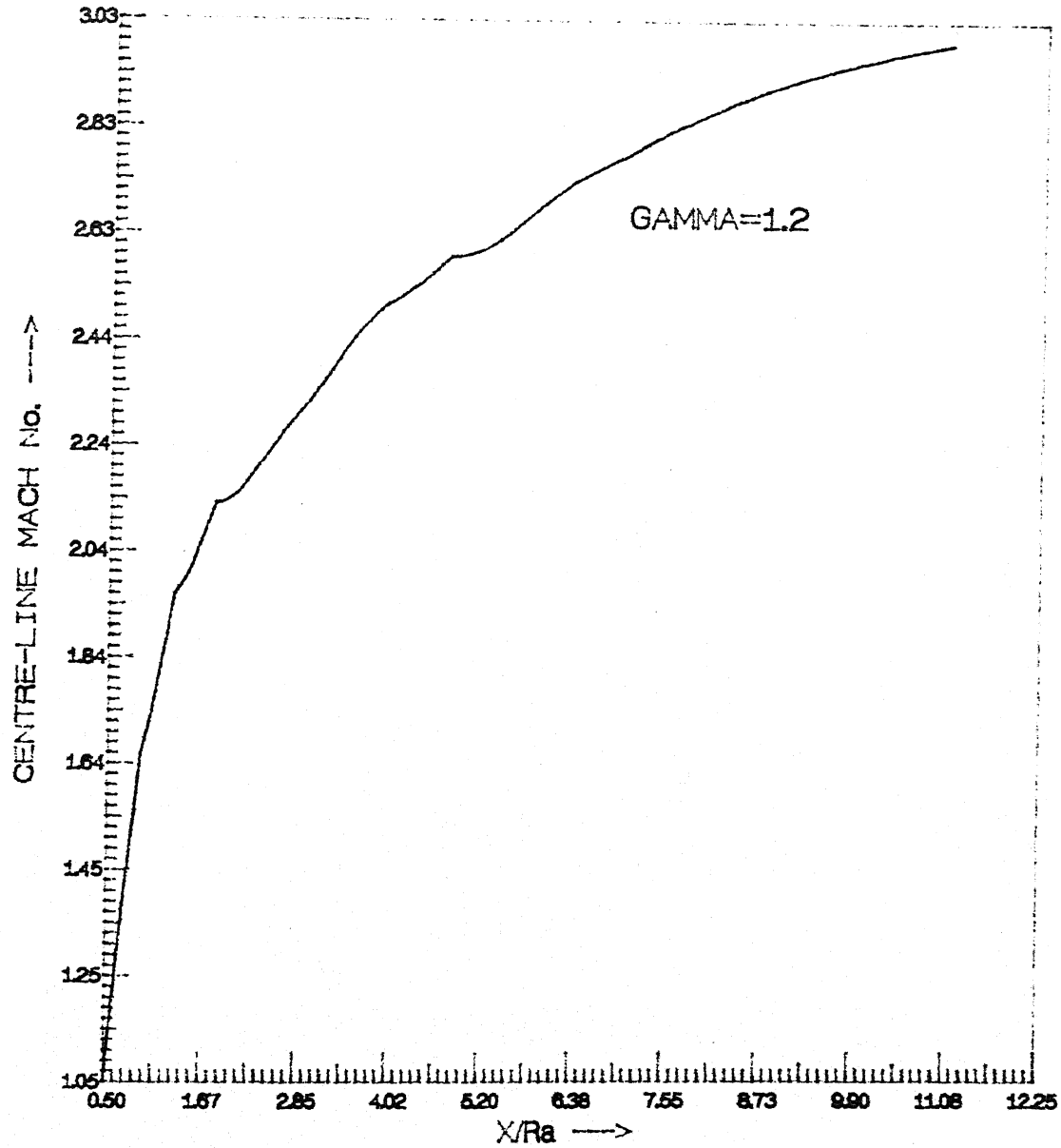

Fig. 29. Centre-line Mach No. distribution for TND-2579 nozzle

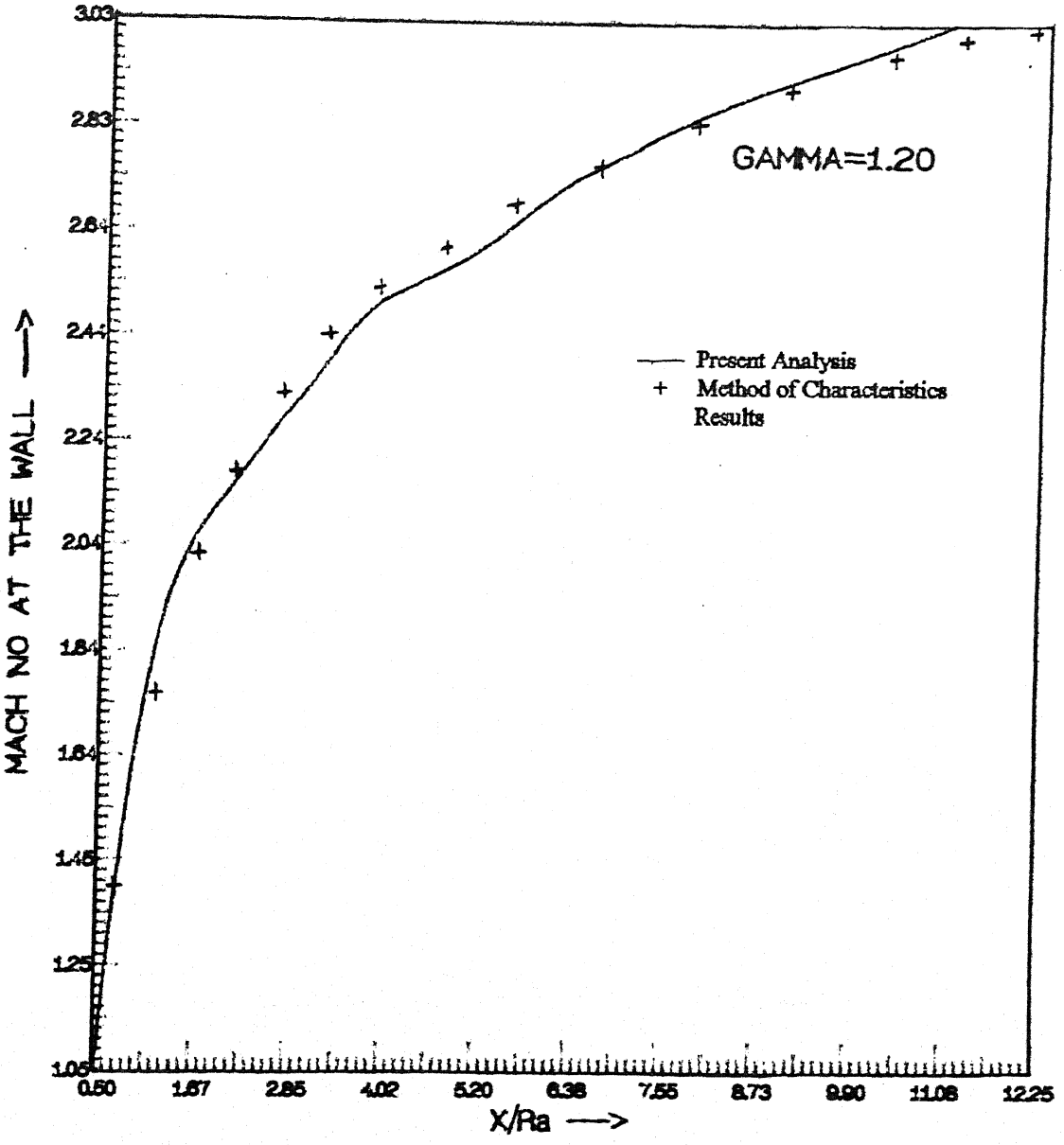

Fig. 30. Wall Mach No. distribution for TND-2579 nozzle

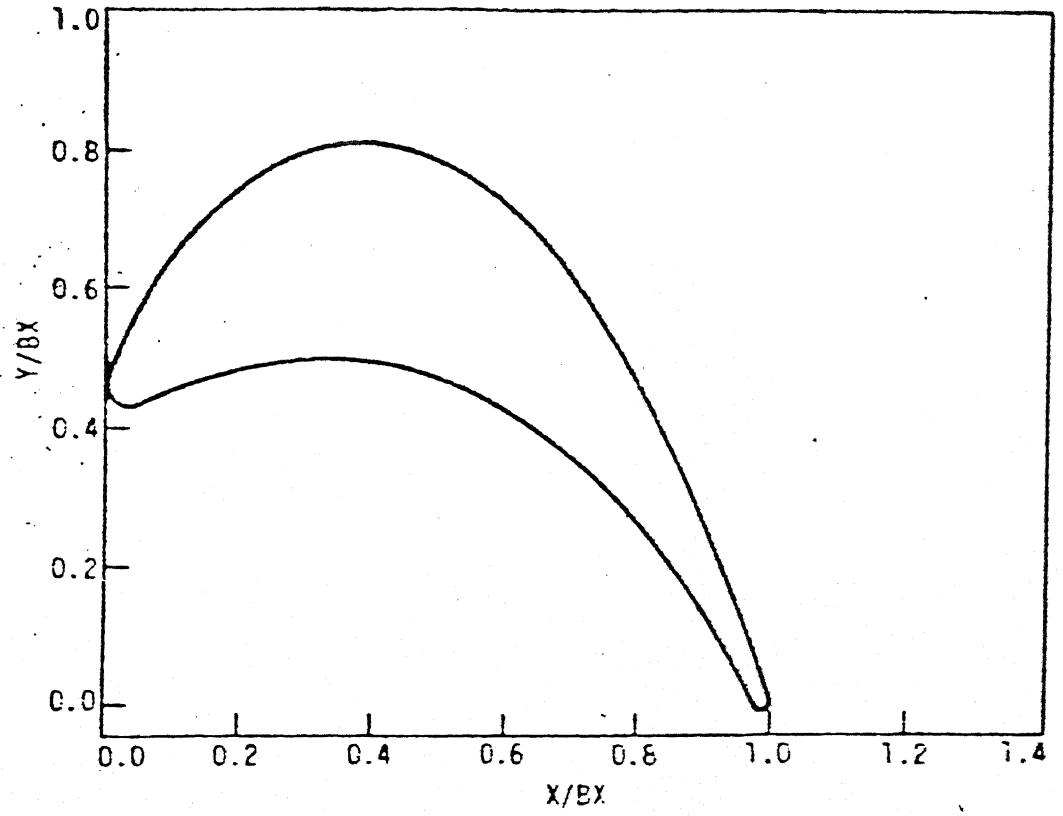

Fig. 31. Cascade flow Airfoil geometry

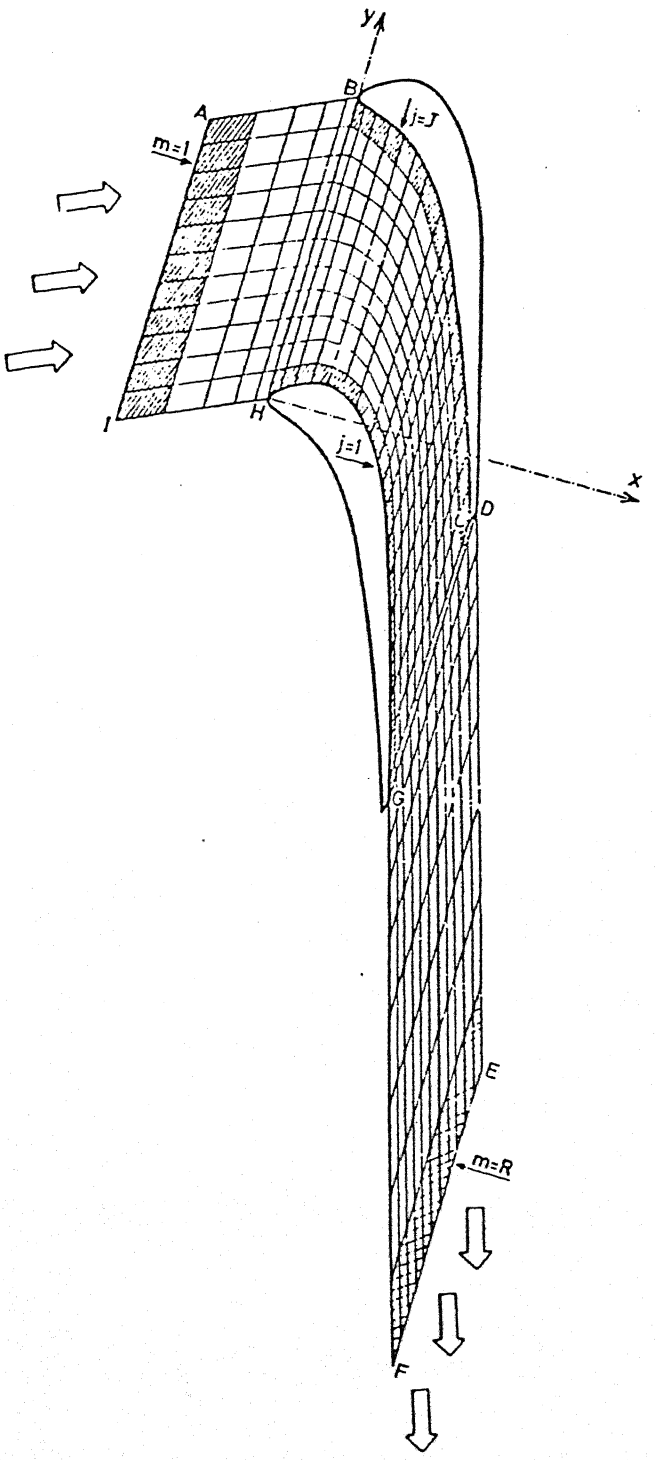

Fig. 32. Cascade flow, typical grid representation

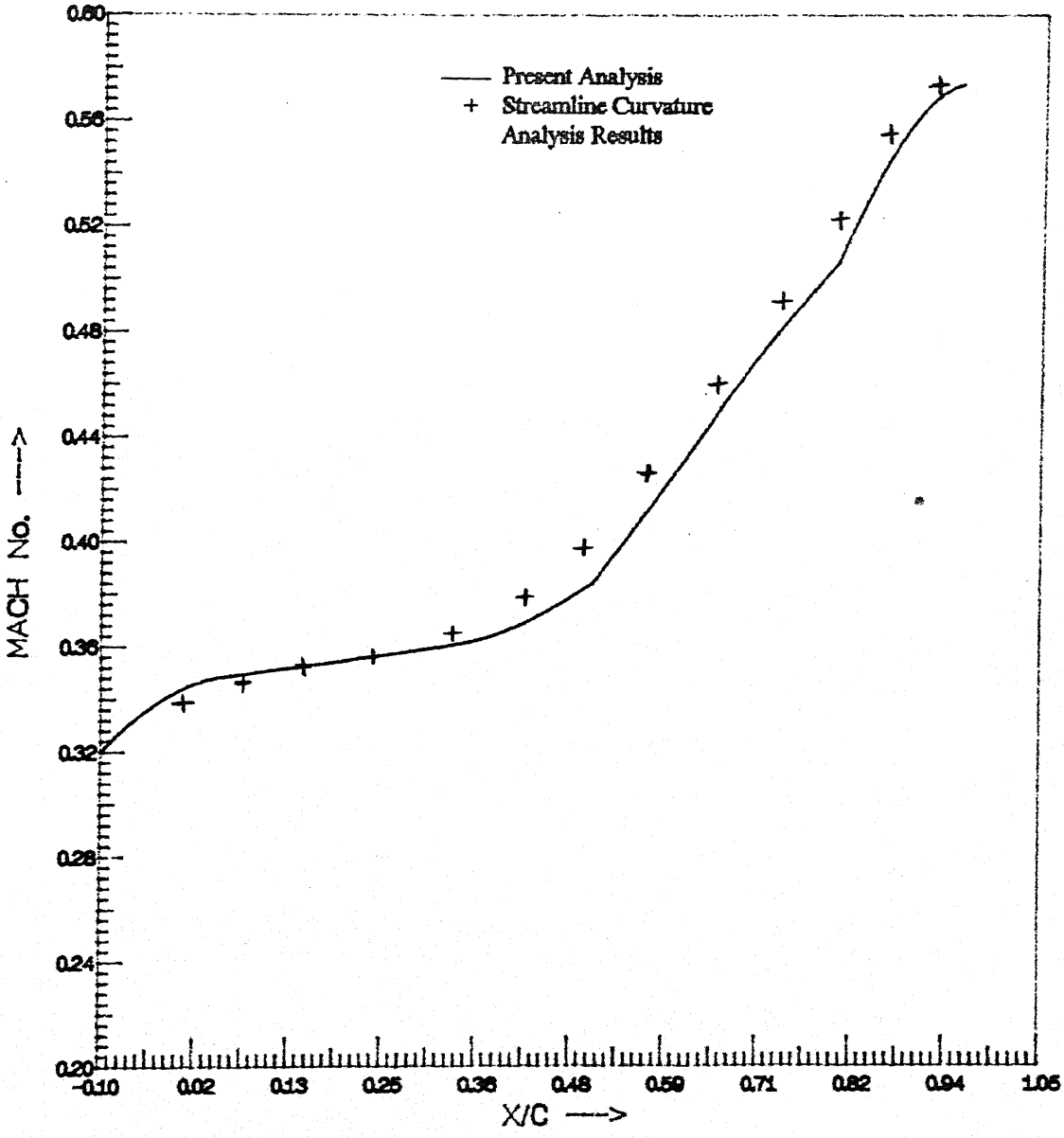

Fig. 33. Centre-line Cascade flow Mach No. distribution

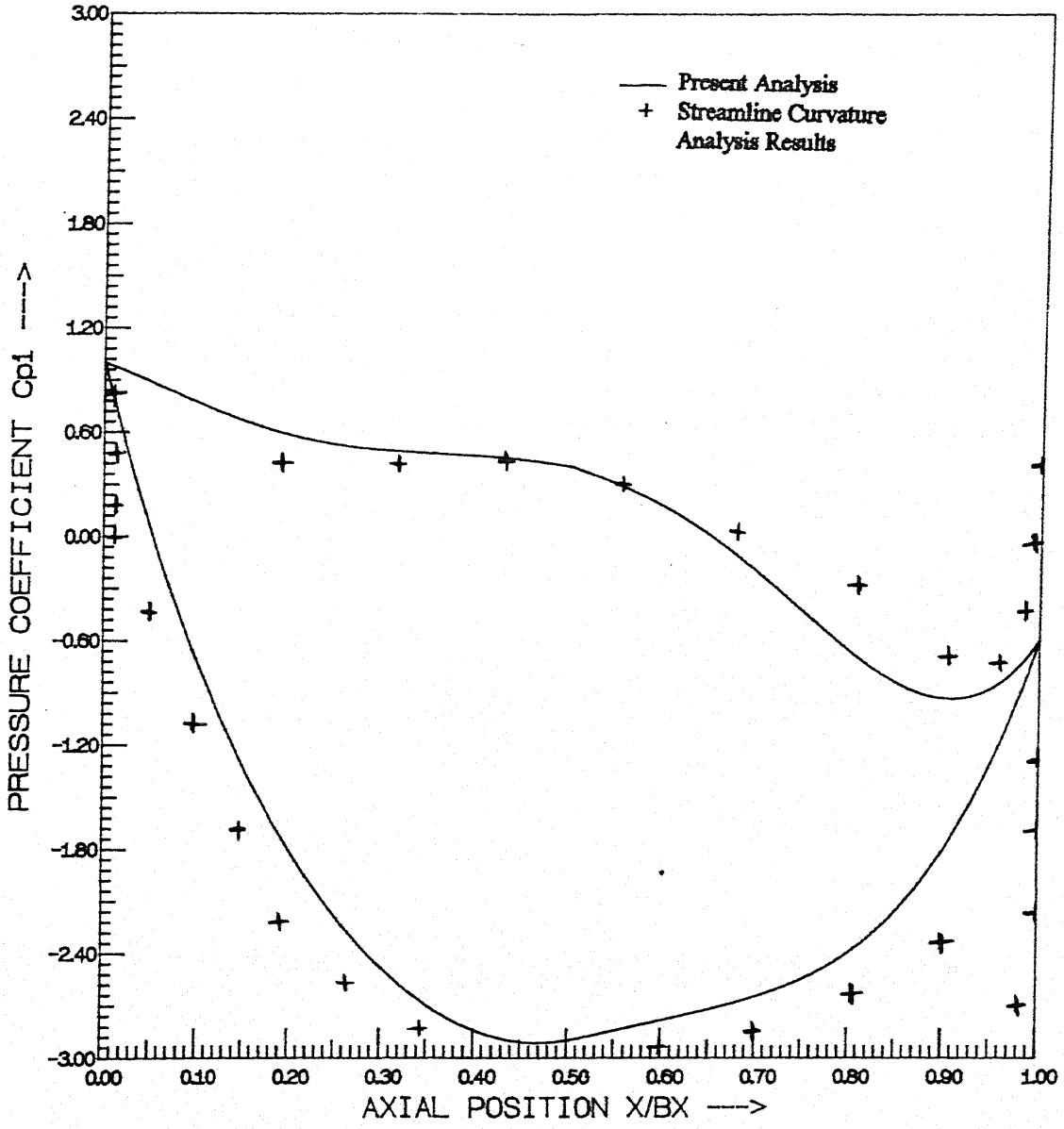

Fig. 34. Cp_i distribution for cascade flow